



**Federal Aviation
Administration**

**Impact of Alternative Jet Fuel and
Fuel Blends on Non-Metallic
Materials Used in Commercial
Aircraft Fuel Systems**

**CLEEN Project Final Report –
Submitted by The Boeing Company**



The Continuous Lower Energy, Emissions and Noise (CLEEN) program is a Federal Aviation Administration NextGen effort to accelerate development of environmentally promising aircraft technologies and sustainable alternative fuels. The CLEEN Program is managed by the FAA's Office of Environment and Energy.

The report presented herein is the final report deliverable submitted by The Boeing Company for a project conducted under the CLEEN Program to examine the impact of alternative jet fuel and fuel blends on non-metallic materials used in commercial aircraft fuel systems. This project was conducted under FAA other transaction agreement (OTA) DTFAWA-10-C-0030.

This is report is report number DOT/FAA/AEE/2012-01 by the FAA's Office of Environment and Energy.

Note to the reader: Boeing refers to these fuels throughout the report as synthetic paraffinic kerosene (SPK). The classification of synthetic paraffinic kerosene encompasses alternative fuels derived from both the Fischer-Tropsch (FT) process and those classified as Hydroprocessed Esters and Fatty Acids (HEFA). Both of these fuel types are approved for use in commercial aviation at up to a 50% blend with petroleum jet fuel.

Alternative Fuels

Final Report

OTA Number: DTFAWA-10-C-0030

July 29, 2011

Prepared by:

The Boeing Company, and
University of Dayton Research Institute

Prepared for:

FAA Office of Environment and Energy



Executive Summary

OTA DTFWA-10-C-00030, “Continuous Lower Energy Emissions and Noise (CLEEN) Technologies Program”; Final Report for Alternative Fuels Task: Impact of SPK Fuels and Fuel Blends on Non-metallic Materials used in Commercial Aircraft Fuel Systems

A study has been completed to examine the overall effect of SPK and SPK fuel blends on non-metallic materials used in commercial aircraft fuel systems. The primary measure of performance was the volume swell of dry source materials immersed in fuel for 40 hours at room temperature. Supporting data was obtained in the form of an analysis of the fuel absorbed by each test material using either thermogravimetric analysis or by thermal desorption gas chromatography-mass spectrometry. The volume swell and fuel absorbed using a set of 12 Jet-As and 4 SPKs were used as the primary basis for comparison. The Jet-As were selected to span a broad range of aromatics (from 8.7% to 23.1%) while the SPKs were selected from a variety of sources, though they were processed into 4 very similar fuels with 0% aromatics. To evaluate the relative importance of the molecular structure of fuel components in general, and aromatics in particular, the activity of 10 aromatics selected to emphasize the relative roles of molar volume, polarity, and hydrogen bonding were measured and compared with the reference Jet-As. Furthermore, data was obtained on a set of fuels consisting of 50% SPK/Jet-A fuel blends to assess the effect of these fuels on fuel system materials regardless of their aromatic content as well as the effect of those blends with 8% aromatics. This work was presented at CRC annual meeting in Seattle in May, 2011, just prior to the updated ASTM D7566-11 fuel specification approval of up to 50% SPK blends, released on July 1, 2011.

The overall response to the aromatic content of the fuel was found to be very material-dependent with the greatest effect being shown by a nitrile rubber O-ring material, a polythioether and a polysulfide sealant. A fluorocarbon O-ring material was found to be relatively inert while two epoxy coatings and a nylon and a Kapton® film were found to be essentially inert in all of the test fuels. A fluorosilicone O-ring material was found to show moderate volume swell behavior, however the volume swell of this material was a very weak function of the aromatic content.

Although the volume swell of the test materials tended to increase with the aromatic of the fuel, only the nitrile rubber O-ring and a polythioether and polysulfide sealant materials showed a volume swell character in the SPKs that was lower than that of Jet-A based on the reference fuels used. It is very important to note that these results should be considered a statistical prediction as to whether the volume swell of a given blend would fall within the predicted ‘normal’ range for Jet-A.

With respect to the influence of the molecular structure of the fuel; volume swell was found to increase as the molar volume of the fuel components decreases and as their polarity and hydrogen bonding increases. Amongst these three factors (molar volume, polarity, hydrogen bonding) molar volume had the least influence on the volume swell followed by polarity and hydrogen bonding. Furthermore, the influence of hydrogen bonding tended to be significantly

higher than that of polarity. This suggests that the volume swell of jet fuel will increase as the boiling range skews towards lower temperatures (lower molecular weight) and as the overall polarity and hydrogen bonding increases, and vice versa. Noting that the bulk of Jet-A and all of typical SPKs are paraffinic and therefore non-polar, the polarity and hydrogen bonding character of the fuel will be dominated by the aromatics. However, emphasizing that the bulk of the fuel is paraffinic, particularly as the aromatic content is lowered, the influence of the molecular weight distribution of the fuel must be considered. This emphasizes the importance of taking into account the composition of a fuel as a whole when considering how it interacts with non-metallic materials and not focusing on one class fraction of the fuel such as aromatic content alone.

Authors:

John L. Graham

University of Dayton Research Institute

Timothy F. Rahmes*, Mark C. Kay, Jean-Philippe Belières, James D. Kinder, Steven A. Millett, Jean Ray, William L. Vannice*

The Boeing Company

*-corresponding authors (Timothy.F.Rahmes@boeing.com, William.L.Vannice@boeing.com)

Table of Contents

| | |
|--|-----|
| Executive Summary | i |
| Table of Contents | iii |
| Index of Tables and Figures..... | iv |
| Figures: (continued) | iv |
| Tables: | vi |
| 1 Introduction and Background | 7 |
| 1.1 Introduction..... | 7 |
| 1.2 Background | 7 |
| 2 Experimental Methods | 10 |
| 2.1 Volume Swell | 10 |
| 2.2 Analysis of Absorbed Fuel | 12 |
| 2.3 Statistical Analysis of the Volume Swell and Mass Fraction of Fuel Absorbed..... | 12 |
| 2.4 Source Materials | 13 |
| 3 Results and Discussion | 15 |
| 3.1 Volume Swell of Reference Jet-A and SPK | 15 |
| 3.2 Thermogravimetric Analysis (Mass Fraction) of Absorbed Fuel | 20 |
| 3.3 GC-MS Analysis of Absorbed Fuel..... | 24 |
| 3.4 Volume Swell of 50% SPK/Jet-A Fuel Blends | 28 |
| 3.5 The Behavior of SPK Blended with Selected Aromatics | 31 |
| 4 Technical Summary | 40 |
| 5 Appendices..... | 42 |
| 5.1 Appendix A N0602 Nitrile Rubber O-Ring..... | 42 |
| 5.2 Appendix B N0602e Extracted Nitrile Rubber O-Ring..... | 45 |
| 5.3 Appendix C L1120 Fluorosilicone O-Ring | 46 |
| 5.4 Appendix D V0835 Fluorocarbon O-ring..... | 48 |
| 5.5 Appendix E PR-1776 Polysulfide Sealant | 50 |
| 5.6 Appendix F PR-1828 Polythioether Sealant..... | 52 |
| 5.7 Appendix G BMS 10-20 Epoxy Fuel Tank Coating..... | 54 |
| 5.8 Appendix H BMS 10-123 Epoxy Fuel Tank Coating..... | 55 |
| 5.9 Appendix I Nylon (6,6) Film | 56 |
| 5.10 Appendix J Kapton® Film..... | 57 |
| 5.11 Appendix K JP-8 to FT Transition | 58 |

Index of Tables and Figures

Figures: (continued)

| | |
|--|----|
| Figure 2-1. Schematic of an optical dilatometer..... | 10 |
| Figure 2-2. An early example of an optical dilatometer..... | 11 |
| Figure 3-1. The volume swell of the O-ring materials after 40 hours at room temperature. Note the relative difference between the average SPK and the Jet-A 90% prediction interval is in parentheses | 17 |
| Figure 3-2. The volume swell of the sealant materials after 40 hours at room temperature. Note the relative difference between the average SPK and the Jet-A 90% prediction interval is in parentheses | 18 |
| Figure 3-3. The volume swell of the coating materials after 40 hours at room temperature. Note the relative difference between the average SPK and the Jet-A 90% prediction interval is in parentheses | 18 |
| Figure 3-4. The volume swell of the film materials after 40 hours at room temperature. Note the relative difference between the average SPK and the Jet-A 90% prediction interval is in parentheses | 19 |
| Figure 3-5. The coefficient of determination (R^2) versus the specific swell (slope of the volume swell in the reference Jet-As versus their aromatic content)..... | 20 |
| Figure 3-6. An example TGA trace for dry nitrile rubber and nitrile rubber aged in a Fischer-Tropsch (FT) fuel showing the mass of plasticizer extracted by the fuel is similar to the mass of fuel absorbed | 21 |
| Figure 3-7. Summary of TGA results for the O-ring materials | 23 |
| Figure 3-8. Summary of TGA results for the sealant materials..... | 24 |
| Figure 3-9. Example chromatograms comparing the fuel absorbed by the nitrile rubber (N0602) O-ring material (top) and the fuel in which they were aged (bottom). Note that normal alkanes are labeled with their carbon number..... | 25 |
| Figure 3-10. Example chromatograms comparing the fuel absorbed by the fluorosilicone (L1120) O-ring material (top) and the fuel in which they were aged (bottom). Note that normal alkanes are labeled with their carbon number..... | 25 |
| Figure 3-11. Example chromatograms comparing the fuel absorbed by the fluorocarbon (V0835) O-ring material (top) and the fuel in which they were aged (bottom). Note that normal alkanes are labeled with their carbon number..... | 26 |
| Figure 3-12. Example chromatograms comparing the fuel absorbed by the polysulfide (PR-1776) sealant material (top) and the fuel in which they were aged (bottom). Note that normal alkanes are labeled with their carbon number..... | 26 |
| Figure 3-13. Example chromatograms comparing the fuel absorbed by the polythioether (PR-1828) material (top) and the fuel in which they were aged (bottom). Note that normal alkanes are labeled with their carbon number..... | 27 |
| Figure 3-14. The volume swell of the O-ring materials after 40 hours at room temperature in the neat reference Jet-As and 50% SPK-/Jet-A blends. | 30 |
| Figure 3-15. The volume swell of the sealant materials after 40 hours at room temperature in the neat reference Jet-As and 50% SPK-/Jet-A blends | 30 |
| Figure 3-16. The volume swell of the coating materials after 40 hours at room temperature in the neat reference Jet-As and 50% SPK-/Jet-A blends | 31 |

| | |
|---|----|
| Figure 3-17. The volume swell of the film materials after 40 hours at room temperature in the neat reference Jet-As and 50% SPK-/Jet-A blends | 31 |
| Figure 3-18. Molecular structures of the aromatic selected for this study..... | 33 |
| Figure 3-19. Specific swell as a function of the molar volume of the aromatic blended with SPK-1 | 36 |
| Figure 3-20. Specific swell as a function of the polar HSP of the aromatic blended with SPK-1 | 36 |
| Figure 3-21. Specific swell as a function of the hydrogen bond HSP of the aromatic blended with SPK-1 | 37 |
| Figure 3-22. Polymer-fuel partition coefficients as a function of the molar volume of the aromatic blended with SPK-1 | 38 |
| Figure 3-23. Polymer-fuel partition coefficients as a function of the polar HSP of the aromatic blended with SPK-1 | 38 |
| Figure 3-24. Polymer-fuel partition coefficients as a function of the hydrogen bond HSP of the aromatic blended with SPK-1 | 39 |
| Figure A-1 Average volume swell as a function of time for N0602 at room temperature | 42 |
| Figure B-1 Average volume swell as a function of time for N0602e at room temperature | 45 |
| Figure C-1 Average volume swell as a function of time for L1120 at room temperature..... | 46 |
| Figure D-1 Average volume swell as a function of time for V0835 at room temperature | 48 |
| Figure E-1 Average volume swell as a function of time for PR-1776 at room temperature | 50 |
| Figure F-1 Average volume swell as a function of time for PR-1828 at room temperature | 52 |
| Figure G-1 Average volume swell as a function of time for BMS 10-20 at room temperature .. | 54 |
| Figure H-1 Average volume swell as a function of time for BMS 10-123 at room temperature | 55 |
| Figure I-1 Average volume swell as a function of time for Nylon (6,6) at room temperature.... | 56 |
| Figure J-1 Average volume swell as a function of time for Kapton® at room temperature | 57 |
| Figure K-1 Volume swell for JP-8 to FT Transition..... | 58 |

Tables:

| | |
|--|----|
| Table 1-1 Hansen Solubility Parameters (MPa ^{1/2}) for Selected Fuel Components | 9 |
| Table 2-1 Fuels Used in This Study..... | 14 |
| Table 2-2 Materials Used in This Study | 14 |
| Table 3-1 Overall Summary of the Volume Swell Results for the Neat Fuels..... | 15 |
| Table 3-2 Average Polymer/Fuel Partition Coefficients | 27 |
| Table 3-3 Estimated Average Composition of Absorbed Fuel..... | 27 |
| Table 3-4 Overlap of the 90% Prediction Intervals for 50% SPK/Jet-A Fuel Blends And 50% SPK/Jet-A Fuel Blends with 8% Aromatic Content | 29 |
| Table 3-5 Aromatics Used in this Study | 32 |
| Table 3-6 Summary of Volume Swell Results for the O-ring and Sealants aged in SPK-1 Blended with Selected Aromatics | 34 |
| Table 3-7 Summary of Volume Swell Results for the Coatings and Films aged in SPK-1 Blended with Selected Aromatics..... | 34 |
| Table 3-8 Summary of Specific Swell Results for the O-ring and Sealants aged in SPK-1 Blended with Selected Aromatics at 8% (unless noted as 3%)..... | 35 |
| Table 3-9 Summary of Specific Swell Results for the Coatings and Films aged in SPK-1 Blended with Selected Aromatics..... | 35 |
| Table 3-10 Summary of Partition Coefficient Results for the O-ring and Sealants aged in SPK-1 Blended with Selected Aromatics | 37 |
| Table A-1 Summary of Volume Swell and Mass Fraction of Fuel Absorbed by N0602..... | 42 |
| Table A-2 Summary of Polymer-Fuel Partition Coefficients (Kpf) for N0602..... | 43 |
| Table A-3 Estimated Composition of the Bulk and Absorbed Fuels..... | 44 |
| Table B-1 Summary of Volume Swell and Mass Fraction of Fuel Absorbed by N0602e | 45 |
| Table C-1 Summary of Volume Swell and Mass Fraction of Fuel Absorbed by L1120..... | 46 |
| Table C-2 Summary of Polymer-Fuel Partition Coefficients (Kpf) for L1120 | 47 |
| Table C-3 Estimated Composition of the Bulk and Absorbed Fuels..... | 47 |
| Table D-1 Summary of Volume Swell and Mass Fraction of Fuel Absorbed by V0835..... | 48 |
| Table D-2 Summary of Polymer-Fuel Partition Coefficients (Kpf) for V0835..... | 49 |
| Table D-3 Estimated Composition of the Bulk and Absorbed Fuels..... | 49 |
| Table E-1 Summary of Volume Swell and Mass Fraction of Fuel Absorbed by PR-1776..... | 50 |
| Table E-2 Summary of Polymer-Fuel Partition Coefficients (Kpf) for PR-1776..... | 51 |
| Table E-3 Estimated Composition of the Bulk and Absorbed Fuels | 51 |
| Table F-1 Summary of Volume Swell and Mass Fraction of Fuel Absorbed by PR-1828 | 52 |
| Table F-2 Summary of Polymer-Fuel Partition Coefficients (Kpf) for PR-1828..... | 53 |
| Table F-3 Estimated Composition of the Bulk and Absorbed Fuels | 53 |
| Table G-1 Summary of Volume Swell and Mass Fraction of Fuel Absorbed by BMS 10-20 | 54 |
| Table H-1 Summary of Volume Swell and Mass Fraction of Fuel Absorbed by BMS 10-123 .. | 55 |
| Table I-1 Summary of Volume Swell and Mass Fraction of Fuel Absorbed by Nylon (6,6)..... | 56 |
| Table J-1 Summary of Volume Swell and Mass Fraction of Fuel Absorbed by Kapton | 57 |

1 Introduction and Background

1.1 Introduction

In 2010 the Federal Aviation Administration (FAA) initiated the Continuous Lower Energy, Emissions and Noise (CLEEN) program to develop technologies to assist in reducing the environmental impact of commercial aviation. One of several technology areas that are being examined for achieving this goal is the use of "drop-in" alternative jet fuels such as synthetic paraffinic kerosene (SPK), which is also known as hydrotreated renewable jet (HRJ). This fuel has the potential to be used in existing engines without modification. SPKs are unique in that they can be obtained from a variety of non-petroleum sources such as coal, natural gas, algae, agriculture, and biomass. The latter are particularly interesting in that they offer the potential for reduced lifecycle greenhouse gas emissions. A significant challenge facing the widespread use of low aromatic jet fuels is fully characterizing the impact of their use in systems that have evolved for use with petroleum distillate fuels. A concern focuses on lower aromatics content in these fuels compared to current fuels in use, which may cause polymeric materials such as O-ring seals and sealants to shrink, harden, and fail. Current industry experience has determined that a minimum of 8% aromatic content is required in synthetic jet fuel blends. Moreover, there is limited knowledge as to the influence of the types of aromatics on the strength of the interaction between the fuel and the various polymeric fuel system materials. However, it is known that while aromatics have a large influence on seal-swell, they are not the only fuel component affecting it. Oxygenates, sulfur-containing compounds, and acidic compounds are some examples of molecules that can also affect materials properties. This report summarizes the results of a study to evaluate the impact of low aromatic jet fuels on the volume swell of selected polymeric materials commonly used in commercial aircraft fuel systems.

1.2 Background

In the absence of chemical reactions, when a new polymeric material is exposed to fuel for the first time two processes can occur. First, the material may absorb components from the fuel (alkanes, aromatics, additives, etc.) which by itself would generally cause the material to swell and soften. (Complete dissolution of the material would be a limiting case of this process.) Second, the fuel may extract components from the material (plasticizers, processing aids, residual solvents, etc.) which would generally cause the material to shrink and harden. The overall effect the fuel has on the material will be the balance of these two processes. Once the material has been in service for some time the fuel-extractable components will have been removed and all subsequent changes in physical properties will result from a shifting equilibrium between the material and the overlying fuel which in turn will depend on the composition of the fuel.

At its most fundamental level, the absorption of fuel by a polymeric material is governed by the chemical physics of polymer solutions, specifically the processes that occur very early in the formation of a polymer solution where the fluid first wets, then penetrates the polymer matrix. Thermodynamically, this process can be described as a series of discrete steps beginning with the

separation of fuel molecules from the bulk fluid through the breaking of fuel-fuel intermolecular bonds. Next, a cavity large enough to accept the fuel molecule must be opened in the polymer by breaking polymer-polymer intermolecular bonds on adjacent polymer strands, a process that imparts elastic strain on the polymer surrounding the penetration site. Finally, the fuel molecule is inserted into the polymer, creating polymer-fuel bonds. (The cavity left behind in the fuel must also be closed, though this step is often disregarded.) Energetically, this process can be expressed as the breaking of fuel-fuel intermolecular bonds (requiring energy), the separation of the polymer-polymer intermolecular bonds (requiring energy), and the making of polymer-fuel intermolecular bonds (releasing energy). Considering the overall energy balance of these processes, the strength of interaction between the fuel and polymer depends on the size and shape of the fuel molecules, the intermolecular bonding of the polymer, the intermolecular bonding of the fuel, and the intermolecular bonds that form between the polymer and the fuel penetrants.

One method of expressing the intermolecular bonding of polymers and solvents (in this case the fuel molecules) is through the use of Hansen solubility parameters (HSPs). Briefly, HSPs summarize the relative contributions of dispersion (van der Waals forces), polarity (dipole-dipole interactions), and hydrogen bonding (specific electrostatic interactions) to the overall intermolecular bonding of pure species (fuel-fuel and polymer-polymer interactions). The HSPs for selected fuel components are summarized in Table 1-1. These show that alkanes tend to be relatively large molecules that are non-polar and do not participate in hydrogen bonds. In contrast, aromatics (alkyl benzenes) are more compact, they can exhibit some polarity and they can form weak hydrogen bonds. The diaromatics (alkyl naphthalenes) are also relatively compact and can exhibit significant polar and hydrogen bonding character. Given that most fuel system polymers obtain their fuel resistance by virtue of relatively high polarity and hydrogen bonding it has been found that in very general terms the strength of interaction between a fuel and a polymeric fuel system material tends to increase as the molar volume of the fuel components decrease and as their polarity and hydrogen bonding increases. Based on these factors, the HSPs listed in Table 1-1 suggest that alkanes will have the weakest interactions with fuel-resistant polymeric materials followed by aromatics and diaromatics, which is consistent with the general observation that physical properties such as volume swell tends to vary with the aromatic content of jet turbine fuels. However, it is important to note that the extent of interaction will be very material dependent as well as a function of the specific components present in the fuel. Furthermore, it is important to note that while the interactions between the alkanes and fuel-resistant materials is expected to be weak, the alkanes are the largest single class of compounds in a typical jet fuel and they can also have an influence on the overall strength of interaction between the fuel and polymer.

With respect to the material compatibility of jet fuels, including alternative fuels, it would be beneficial if there were tabulations of the allowable limits function critical physical properties (volume change, modulus, glass transition temperature, etc.) but unfortunately this information is not available. This is a consequence of the historical background of how fuel system materials have been developed; that is the implicit assumption that they would be used in service with petroleum distillate fuels whose properties are set by the respective fuel specifications which in turn limits the variation in both composition and the range of interactions these fuel have on

polymeric materials. In the absence of defensible, quantitative limits on physical properties an alternative approach to assessing material compatibility has been developed. Briefly, it is assumed that all fuel system materials currently in use have passed their respective qualification requirements and no further certification is necessary. Furthermore, in the course of normal service fuel system polymers are exposed to a variety of fuels with a commensurate range of compositions and range of interactions with the fuel system materials. By default, even though the range of the real in-service variation in the physical properties of these polymers may be unknown, they are considered acceptable by virtue of the fact that they do not adversely affect current in-service performance. Consequently, the overall approach used in this study is to establish a reference population using a set of representative jet fuels and to compare the behavior of the test fuels and fuel blends with this reference set. If the variation of the selected physical property resulting from the exposure to the test fuel falls within the range of the reference population then the test fuel is likely to be compatible with conventional fuels. If the variation of the physical property resulting from the exposure to the test fuel falls outside the range of the reference population the extent of deviation can form the basis for making a determination as the material compatibility of the test fuel.

Table 1-1 Hansen Solubility Parameters (MPa^{1/2}) for Selected Fuel Components

| Compound Class | Fuel Component | Hansen Solubility Parameters | | | MV mL/mol |
|--------------------|-------------------------|------------------------------|-------|--------|--------------|
| | | Dispersion | Polar | H-Bond | |
| Alkanes | Nonane | 15.7 | 0.0 | 0.0 | 180 |
| | Decane | 15.7 | 0.0 | 0.0 | 196 |
| | Dodecane | 16.0 | 0.0 | 0.0 | 229 |
| | Hexadecane | 16.3 | 0.0 | 0.0 | 294 |
| Aromatics | Benzene | 18.4 | 0.0 | 2.0 | 89 |
| | Toluene | 18.0 | 1.4 | 2.0 | 107 |
| | o-Xylene | 17.8 | 1.0 | 3.1 | 121 |
| | Ethyl Benzene | 17.8 | 0.6 | 1.4 | 123 |
| | 1,2,3-Trimethylbenzene | 17.8 | 0.4 | 1.0 | 134 |
| | 1,3,5-Trimethyl Benzene | 18.0 | 0.0 | 0.6 | 140 |
| | o-Diethyl Benzene | 17.7 | 0.1 | 1.0 | 154 |
| | p-Diethyl Benzene | 18.0 | 0.0 | 0.6 | 157 |
| | N-Butylbenzene | 17.4 | 0.1 | 1.1 | 157 |
| | o-N-Butyltoluene | 17.6 | 0.1 | 1.0 | 171 |
| | p-N-Butyltoluene | 17.4 | 0.1 | 1.0 | 174 |
| Diaromatics | Naphthalene | 19.2 | 2.0 | 5.9 | 112 |
| | 1-Methyl Naphthalene | 20.6 | 0.8 | 4.7 | 139 |

2 Experimental Methods

2.1 Volume Swell

The physical property of fuel system materials selected for analysis in this study is volume swell. Volume swell is a basic response of a polymeric material when exposed to jet fuel and an important physical property for components such as O-ring seals, sealants, and coatings. Volume swell was measured using a technique described as optical dilatometry (see J.L. Graham, R.C. Striebich, K.J. Myers, D.K. Minus, W.E. Harrison, "The Swelling of Nitrile Rubber by Selected Aromatics Blended in a Synthetic Jet Fuel," *Energy and Fuels*, 20 (2), 2006, pp. 759-765). As illustrated in Figure 2-1, and shown in Figure 2-2 an optical dilatometer consists of an optical cell positioned over a small digital camera and illuminated from above with a small flat panel LED. For each analysis small samples measuring approximately 2mm x 2mm were placed in the optical cell along with 10 mL of the test fuel. (As described below and listed in Table 2-2, the thickness of the samples varied depending on the source material.) The samples were positioned near the center of the cell and rested on the bottom of the vessel. Starting at 2 minutes after being immersed in the fuel the samples were digitally photographed every 20 seconds for the next 3 minutes. At 6 minutes total elapsed time the samples were photographed every 15 minutes for the next 40 hours. During the exposure the fuel was static and at room temperature (75°F +/- 5°F). After the aging period was complete the cross-sectional area of each sample was extracted from the digital images, which in turn was taken as a characteristic dimension proportional to the volume (isotropic volume swell was assumed for the amorphous materials used here). The final volume swell for each sample is taken as the average of the last five data points in each set (the last hour of the exposure). The final volume swell for each test material is taken as the average of 2 or more samples.

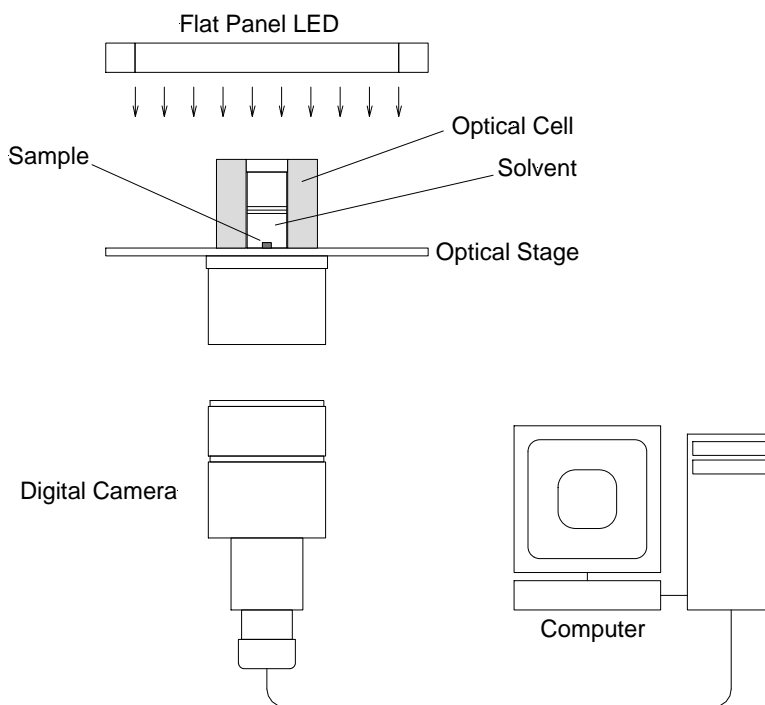


Figure 2-1. Schematic of an optical dilatometer.



Figure 2-2. An early example of an optical dilatometer.

Note that in some cases (see the appendices) the volume swell of the test material was not at equilibrium by the end of the 40-hour aging period. However, the progression of the volume swell was considered sufficient to establish the relative response of each material to the test fuel. Furthermore, the scope of this study was intended to examine the acute response of the test materials to each of the test fuels.

2.2 Analysis of Absorbed Fuel

Although volume swell was the primary measure of a material's overall response to a fuel, additional supporting data in the form of the mass fraction of fuel absorbed as measured by thermogravimetric analysis (TGA) as well as the composition of the absorbed fuel as determined by gas chromatography-mass spectrometry (GC-MS). For the latter the composition of the absorbed fuel is determined by direct thermal desorption GC-MS of small samples weighing approximately 1mg sectioned from the volume swell samples and returned to the fuel for 7-10 days. An identical analysis was performed on the fuel in which the material was aged allowing the relative solubility of the major class fractions of the fuel to be expressed in terms of their partition coefficients (K_{pf}, the ratio of the concentration in the material to the concentration in the overlying fuel). The K_{pf} values reflect the relative solubility of each class fraction in the specific test material. The K_{pf} values were also used to estimate the overall composition of the absorbed fuel to reflect how each class fraction contributes to the observed volume swell. For this study the major class fractions were taken as the alkanes, aromatics (alkyl benzenes), naphthalene, and naphthalenes (alkyl naphthalenes). These class fractions are obtained from the total ion chromatograms (TICs) using extracted ions taken as being characteristic of each class; 43 amu (atomic mass units) for the alkanes, 105 amu for the alkyl benzenes, 128 amu for naphthalene, and 141 amu for the alkyl naphthalenes.

2.3 Statistical Analysis of the Volume Swell and Mass Fraction of Fuel Absorbed

Once the volume swell and mass fraction of fuel absorbed had been obtained for all of the reference Jet-A's the mean (using a linear fit to the data), 90% confidence interval, and 90% prediction interval for all Jet-A's with an aromatic content of 10%-25% was estimated using SAS v9.2 (SAS Institute, Inc.). Although 8% has been proposed as a lower limit for the aromatic content of alternative jet turbine fuels, the range of 10%-25% was selected as being representative of the range in which 95% of all jet turbine fuels lie based on an analysis of JP-8 purchased by the U.S. Air Force (see "Properties of Fischer-Tropsch (FT) Fuel Blends for Use in Military Equipment", SAE Document Number 2006-01-0702). This approach results in an analysis that is somewhat more conservative than the proposed 8% lower limit.

In addition to describing the statistical distribution of the reference populations, a similar analysis was applied to 50% SPK/Jet-A fuel blends. The overlap between the 90% prediction intervals (P.I.) of the reference and test fuel populations was taken as;

$$\text{Overlap 90\% PI} = \frac{(\text{UL Test Fuel}) - (\text{LL Reference Fuels})}{(\text{UL Test Fuel}) - (\text{LL Test Fuel})} \times 100\% \quad (1)$$

Here UL and LL are the upper limit and lower limit of the respective 90% confidence intervals. A similar metric was used to quantify the relative difference between the average point values for the SPKs and the reference populations as;

$$\text{Relative Difference} = \frac{(\text{Point Value}) - (\text{LL Reference Fuels})}{(\text{UL Reference Fuels}) - (\text{LL Reference Fuels})} \times 100\% \quad (2)$$

Finally, each of the reference data sets was fit with a linear regression model of the volume swell versus the aromatic content of the fuel and summarized in terms of the intercept (estimated volume swell in a Jet-A with 0% aromatics), slope (also referred to as the specific swell; %swell/%aromatics), and coefficient of determination (R^2).

2.4 Source Materials

The fuels selected for use in this study are listed in Table 2-1. These included 12 Jet-A fuels with 8.7% to 23.1% aromatics. All reference fuels used were taken from commercial providers, without modification, with the exception of the lowest aromatic sample (SRI-1), which, after clay treating was examined for the presence of residual diEGME using extracted ion chromatograms taking mass fragments with m/e of 45 and 90 amu as being characteristic of this additive. This analysis showed that if present, diEGME in SRI-1 was below the detection limit of approximately 1 ppm. Furthermore, the fuel absorbed by each elastomer was also examined for the presence of diEGME and none was observed.

The materials selected for these are listed in Table 2-2, and included 4 O-ring materials, 2 sealants, 2 coatings, and 2 films. Note that the nitrile rubber material was examined in two variants; as-received N0602 and as a version with its plasticizer extracted and re-designated as N0602e. Briefly, the N0602e O-ring samples were prepared by soaking them in acetone for 24 hours, rinsing them with fresh acetone, and repeated 3 times. After the final wash with fresh acetone the samples were air-dried for 24 hours, then dried in a force-convection oven at 60°C for 1 hour.

Table 2-1 Fuels Used in This Study

| Fuel | ID | Aromatics | Naphthalenes | Notes |
|---------|-------|-----------|--------------|-------------------------|
| Jet-A | SRI-1 | 8.7% | 0.2% | Clay-treated JP-8 |
| | 4597 | 15.0% | 1.9% | |
| | 5245 | 15.5% | 0.2% | |
| | 3166 | 17.6% | 2.5% | |
| | 4598 | 17.6% | 1.4% | |
| | 4600 | 17.7% | 1.3% | |
| | 4658 | 17.7% | 1.3% | |
| | 4626 | 17.9% | 0.6% | |
| | 5661 | 18.1% | 0.6% | |
| | 4877 | 19.6% | 0.4% | |
| | 4599 | 19.9% | 1.4% | |
| | 3602 | 23.1% | 1.1% | |
| Average | | 17.4% | 1.1% | |
| SPK | SPK-1 | 0.0% | 0.0% | Jatropha |
| | SPK-2 | 0.0% | 0.0% | Camelina |
| | SPK-3 | 0.0% | 0.0% | Jatropha-Camelina-Algae |
| | SPK-4 | 0.0% | 0.0% | Bio-Oil Derived SPK |

*Naphthalenes, **Synthetic Paraffinic Kerosene

Table 2-2 Materials Used in This Study

| Component | Material | Sample ID | Sample Thickness |
|-----------|---------------------------|------------|------------------|
| O-Rings | Nitrile Rubber | N0602 | 1mm |
| | Extracted Nitrile Rubber* | N0602e | 1mm |
| | Fluorosilicone | L1120 | 1mm |
| | Low Temp Fluorocarbon | V0835 | 1mm |
| Sealants | Lightweight Polysulfide | PR 1776 | 1mm |
| | Polythioether | PR 1828 | 1mm |
| Coatings | Epoxy | BMS 10-20 | 0.2mm |
| | Epoxy | BMS 10-123 | 0.04mm |
| Films | Nylon (6,6) | Nylon | 1mm |
| | Kapton | Kapton | 0.08mm |

3 Results and Discussion

3.1 Volume Swell of Reference Jet-A and SPK

The volume swell of the test materials in the reference fuels and SPKs are summarized in Table 3-1 and Figure 3-1. through Figure 3-4. Each of the data figures shows the average volume swell for each of the test fuels and the 90% confidence interval for each data point (i.e. error bars). The overall statistical analysis includes the line of best fit through the reference data set and the 90% confidence interval for the regression line. The analysis also shows the 90% prediction interval which is a statistical prediction for the volume swell of 90% of all individual Jet-As based on the distribution of the reference fuels. Each graph gives the equation for the line of best fit and the coefficient of determination (R^2). The intercept of this line gives the statistical prediction of the volume swell of a Jet-A with 0% aromatics (the volume swell of the alkane fraction of the fuel in the absence of aromatics), the average strength of interaction between Jet-A and the test material in terms of the slope (specific swell), and how strongly the strength of interaction correlates with the aromatic content of the fuel (the R^2 value).

Table 3-1 Overall Summary of the Volume Swell Results for the Neat Fuels

| Component | Sample ID | Material | Jet-A 90% PI* | | Average SPK | Relative Diff. | Specific Swell** | R^2 |
|-----------|------------|----------------|---------------|--------|-------------|----------------|------------------|-------|
| | | | LL | UL | | | | |
| O-Rings | N0602 | Nitrile Rubber | 3.72% | 17.40% | 0.15% | -26% | 0.549 | 0.724 |
| | N0602e | Nitrile Rubber | 15.25% | 33.24% | 9.98% | -29% | 0.690 | 0.679 |
| | L1120 | Fluorosilicone | 4.00% | 8.03% | 6.44% | 60% | 0.057 | 0.076 |
| | V0835 | Fluorocarbon | 0.18% | 1.30% | 0.25% | 7% | 0.024 | 0.201 |
| Sealants | PR 1776 | Polysulfide | -2.20% | 0.98% | -2.56% | -11% | 0.102 | 0.498 |
| | PR 1828 | Polythioether | 2.00% | 6.85% | 0.17% | -38% | 0.153 | 0.481 |
| Coatings | BMS 10-20 | Epoxy | -0.17% | 0.19% | -0.03% | 39% | -0.005 | 0.071 |
| | BMS 10-123 | Epoxy | -0.14% | 0.18% | -0.03% | 35% | 0.000 | 0.000 |
| Films | Nylon | Nylon | -0.32% | 0.15% | -0.14% | 39% | -0.014 | 0.406 |
| | Kapton | Kapton | -0.21% | 0.20% | -0.14% | 16% | 0.006 | 0.073 |

*PI = Prediction Interval, **Specific Swell = Slope of Volume Swell vs. Aromatic Content

Considering the four O-ring materials (Figure 3-1.), the nitrile rubbers show the strongest response (dependence) to the aromatic content in the reference Jet-As. Specifically, the 90% prediction interval for the as-received nitrile rubber (Figure 3-1.) varies from 3.7% to 17.4% (a span of 13.7%) while the extracted nitrile rubber varies from 15.3% to 33.2% (a span of 18.0%). The slightly wider span of the extracted nitrile rubber is thought to result from the partial extraction of plasticizer from the as-received nitrile rubber by the jet fuel. Specifically, as the aromatic content of the fuel increases, it becomes a better solvent for the plasticizer which tends to depress the volume swell line for the new O-ring material. This effect is absent from the extracted nitrile rubber which is thought to give a better representation of the behavior on in-service nitrile rubber O-rings. Both of the nitrile rubber materials show a strong influence from the aromatics present in the reference fuels with specific swells of 0.549 and 0.690 for the as-received and extracted nitrile rubbers, respectively. Both show modest correlation between the

volume swell and the aromatic content with R^2 values of 0.724 and 0.679 for the as-received and extracted nitrile rubbers, respectively. Note that the 90% confidence intervals on the individual data points is quite small showing that the variation in the data is largely due to real differences in the volume swell character of the different fuels. Finally, note that the volume swell of the SPKs is below the range predicted for Jet-A indicating that the volume swell of the neat SPKs (0% aromatics) would be lower than what is expected with a low-aromatic jet fuel.

The fluorosilicone O-ring material was interesting in that it shows moderate volume swell (from 4 to 8% based on the 90% prediction interval), but only a weak dependence on the aromatic content of the fuel. The specific swell was found to be only 0.0569 with an R^2 value of 0.0764. Furthermore, the average volume swell for the SPKs was found to be near the average for the reference Jet-As; 6.4% for the average of the four SPKs versus 6.0% for the average of the 12 Jet-As. The 90% confidence intervals for the individual data points are much wider than what was observed for the nitrile rubber, though this is typical for this material. Additional data would likely reduce the 90% confidence intervals, however the overall conclusion is not expected to change; fluorosilicone O-rings should be suitable for service in both Jet-A and the SPKs used here.

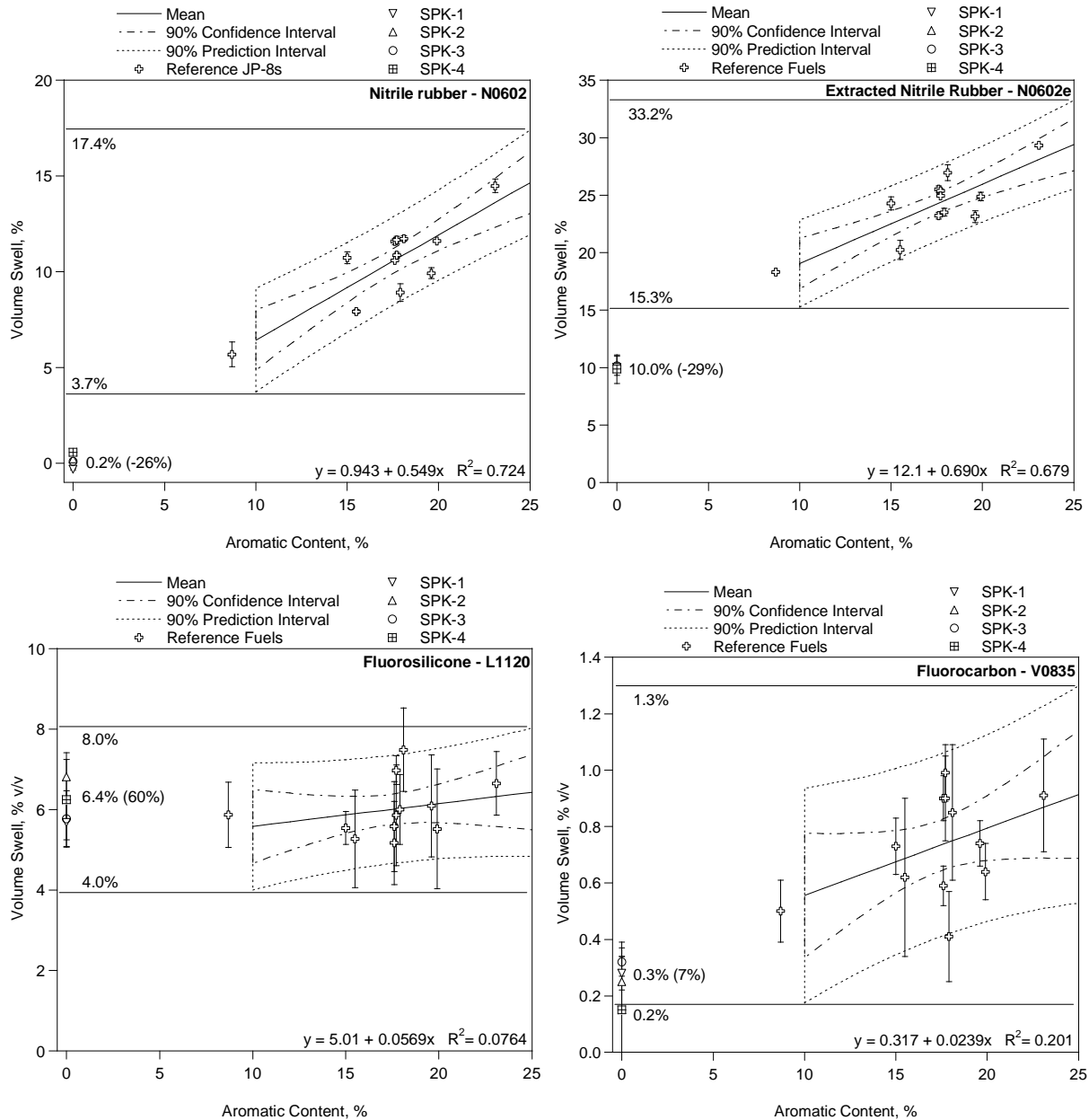


Figure 3-1. The volume swell of the O-ring materials after 40 hours at room temperature. Note the relative difference between the average SPK and the Jet-A 90% prediction interval is in parentheses

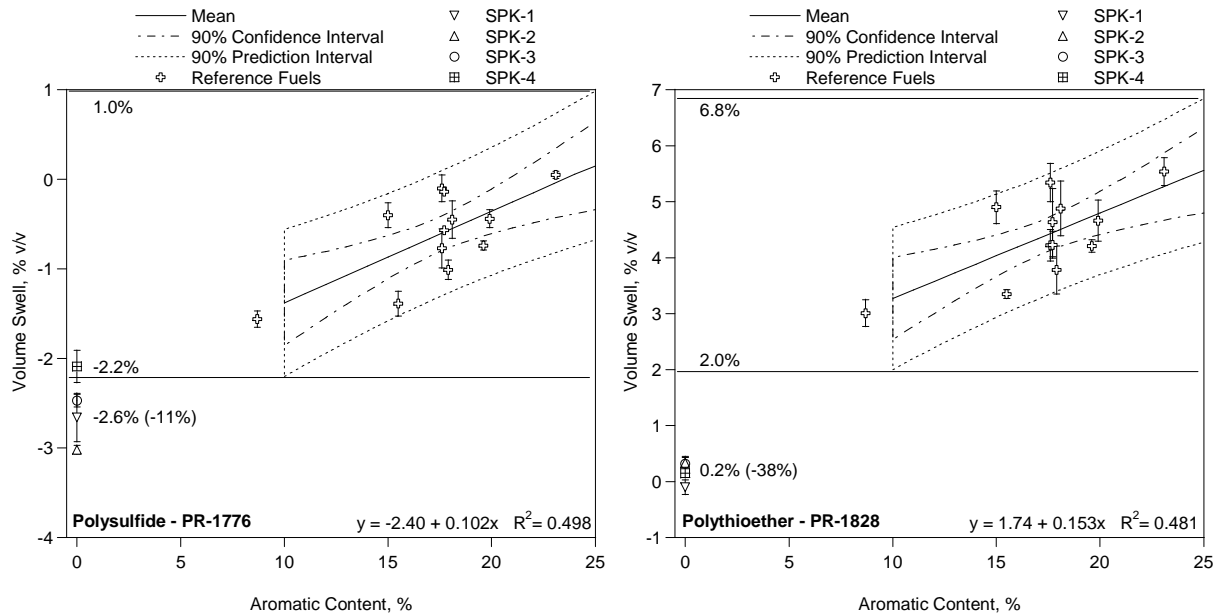


Figure 3-2. The volume swell of the sealant materials after 40 hours at room temperature. Note the relative difference between the average SPK and the Jet-A 90% prediction interval is in parentheses

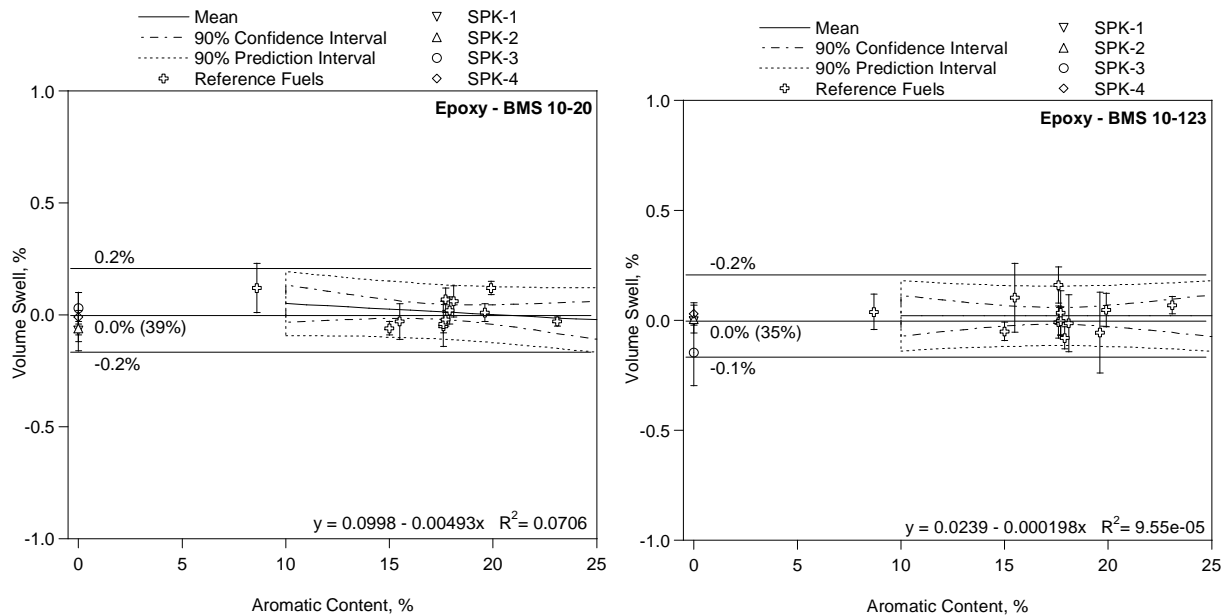


Figure 3-3. The volume swell of the coating materials after 40 hours at room temperature. Note the relative difference between the average SPK and the Jet-A 90% prediction interval is in parentheses

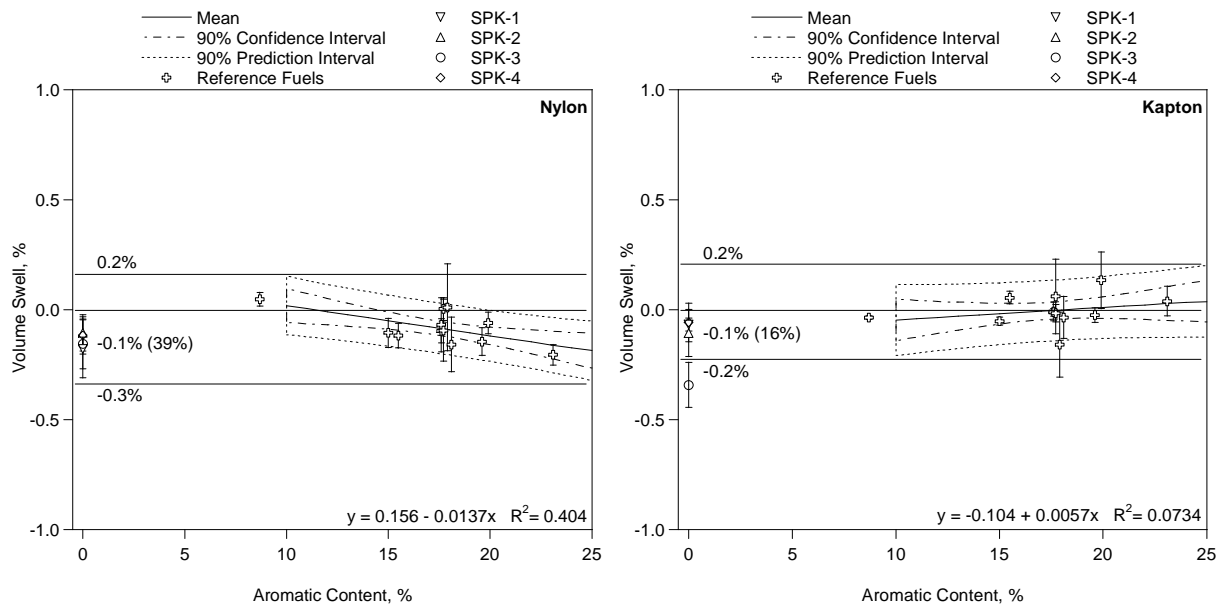


Figure 3-4. The volume swell of the film materials after 40 hours at room temperature. Note the relative difference between the average SPK and the Jet-A 90% prediction interval is in parentheses

The volume swell of the fluorocarbon was found not only to be a relatively weak function of the aromatic content but also to span a relatively narrow range. Specifically, the 90% prediction interval for the volume swell was found to vary from 0.2% to 1.3% with a specific swell of 0.0239 and an R^2 value of 0.201. The average volume swell for the SPKs was found to be within the lower bound of this range with a value of 0.3% suggesting that fluorocarbon O-rings should be suitable for service in both Jet-A and the SPKs used here.

The two sealants showed an interesting range of behavior (Figure 3-2) with the polysulfide PR-1776 shrinking in most of the test fuels and the polythioether showing behavior that was similar to nitrile rubber. The polysulfide showed a modest response to the aromatic content of the reference fuels with the 90% prediction interval varying from -2.2% to 1.0% (a span of 3.2%) and a specific swell of 0.102 and an R^2 value of 0.498. The polythioether showed a somewhat stronger response with the 90% prediction interval varying from 2.0% to 6.8% (a span of 4.8%) and a specific swell of 0.153 and an R^2 value of 0.481. In both materials the volume swell of the SPKs was below the 90% prediction intervals for Jet-A indicating that these materials would shrink to some extent if exposed to these SPKs after being in service with Jet-A, however, given that the polysulfide shrinks even when exposed to Jet-A it is not clear if this would be a problematic response for these materials.

The two coatings and two films (Figure 3-3 and Figure 3-4, respectively) proved to be relatively inert when exposed to the Jet-As and SPKs used in this study. Furthermore, in each case the average volume swell of the SPKs was within range of the reference Jet-As indicating that these materials should be suitable for service in both Jet-A and the SPKs used here.

The overall results from the analysis of the volume swell of the test materials in the reference fuels and neat SPKs is summarized in Table 3-1 and Figure 3-5 in terms of the R^2 values and the specific swell. In this figure the strength of interaction between the fuel and material increases from left to right and the strength of the correlation between the effect and the aromatic content increases from bottom to top. Therefore, materials to the upper right are of highest importance as they show a strong effect that correlates with the aromatic content, while those in the lower left show a relatively weak effect and a poor correlation with the aromatic content. This shows that amongst the materials tested here the nitrile rubbers and sealants are of highest concern for service in low aromatic fuels.

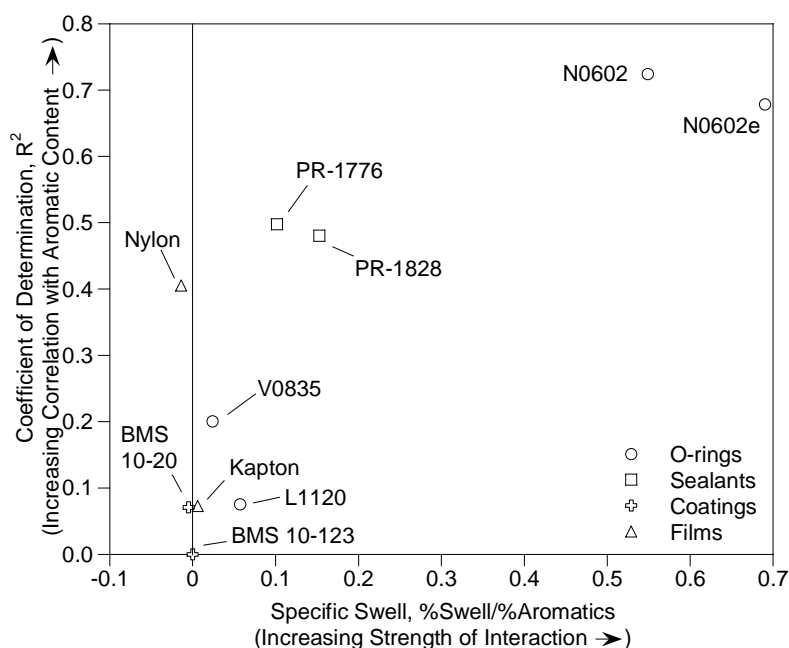


Figure 3-5. The coefficient of determination (R^2) versus the specific swell (slope of the volume swell in the reference Jet-As versus their aromatic content)

3.2 Thermogravimetric Analysis (Mass Fraction) of Absorbed Fuel

The volume swell measurements described above provide valuable information as to how each material responds to the test fuels. However, by itself, volume swell may not accurately reflect the true strength of interaction between the fuel and polymer. Of particular concern are those materials that contain a significant fraction of components such as plasticizers, processing aids, oligomers (partially cured elastomers), and residual solvents that may be extracted by the fuel. For these materials the volume swell measurement may be a convolution of volume gained by the absorption of fuel and volume lost by the extraction of mobile components. This is very common in O-ring materials such as nitrile rubber which is why the plasticizer was removed for one of the materials used in this study. Another very good example is the PR-1776 polysulfide sealant; since this material shrank in nearly all of the fuels used in this study the true strength of

interaction between the fuel and polymer cannot be assessed by the volume swell alone. Another factor is how to evaluate materials for which measuring the volume swell is problematic; materials such as foams and non-curing groove sealants being examples. For these materials an alternative method for measuring the strength of interaction between the fuel and material may be needed.

An alternative to volume swell (or as a supplement to volume swell) is to measure the mass fraction of fuel absorbed by a material using thermogravimetric analysis (TGA). An example of such an analysis is shown in Figure 3-6.

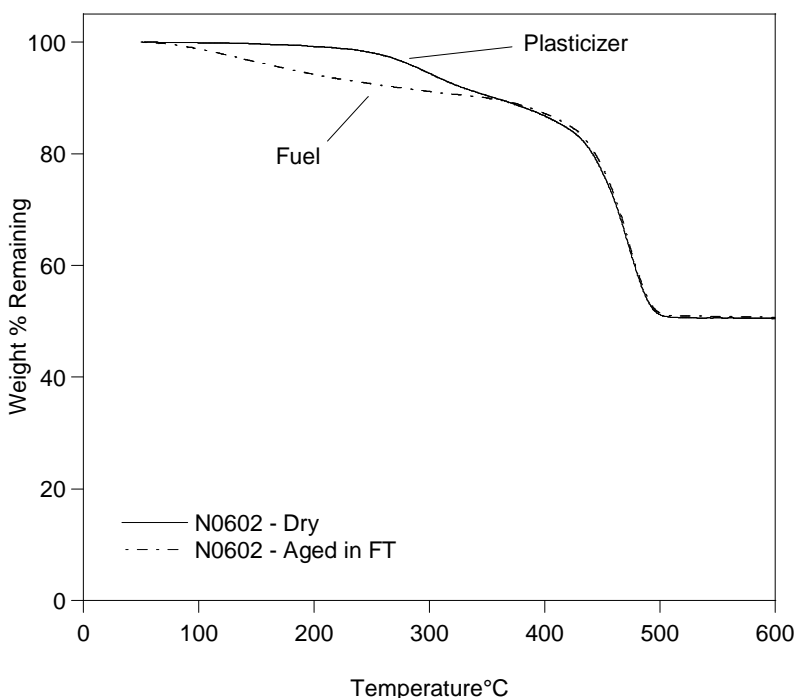


Figure 3-6. An example TGA trace for dry nitrile rubber and nitrile rubber aged in a Fischer-Tropsch (FT) fuel showing the mass of plasticizer extracted by the fuel is similar to the mass of fuel absorbed

The TGA results for the O-ring and sealant materials are summarized in Figure 3-7 and Figure 3-8, respectively. (Note that the coatings and films did not absorb enough fuel to be analyzed by this method). Comparing the TGA and volume swell data shows that the two approaches give very similar results with respect to comparing the mass fraction of the SPK fuel absorbed with the 90% prediction intervals for the mass fraction of Jet-A absorbed. However, there are some informative differences. For example, the results compare very well for the materials that do not have a significant extractable fraction. This includes the extracted nitrile rubber, fluorosilicone, and fluorocarbon O-ring materials. This is because the volume fraction and mass fraction of fuel absorbed are related through the density of the polymer and fuel so that while the two methods may give numerically different results, the comparative results should be the same. For materials that do have a significant extractable fraction the TGA results compare well with the volume

swell results in terms of comparing the SPK and reference Jet-As, however the TGA results more accurately reflect the true strength of interaction between the fuels and elastomers. For example, the volume swell results for the as-received nitrile rubber (Figure 3-1.) shows only 0.2% volume swell for the average SPKs suggesting that only 0.2% v/v fuel is absorbed and that the interaction between the SPKs and nitrile rubber was very weak. However, the TGA results show that 6.4% m/m fuel was actually being absorbed indicating a much stronger level of interaction between the SPK and nitrile rubber. Similarly, the volume swell data for the PR-1828 polythioether also showed an average of only 0.2% v/v, but the TGA data showed an average of 1.3% m/m of the SPKs were being absorbed. Finally, since nearly all of the PR-1776 polysulfide samples shrank when exposed to the SPKs and Jet-As this data reveals very little about the true strength of interaction between the fuels and this material. However, the TGA data shows that an average of 2.0% m/m of the SPKs was being absorbed by this material. Finally, by comparing the TGA results for the as-received and extracted nitrile rubbers (Figure 3-7) shows that removing the plasticizer did not affect the absorption of fuel by this material.

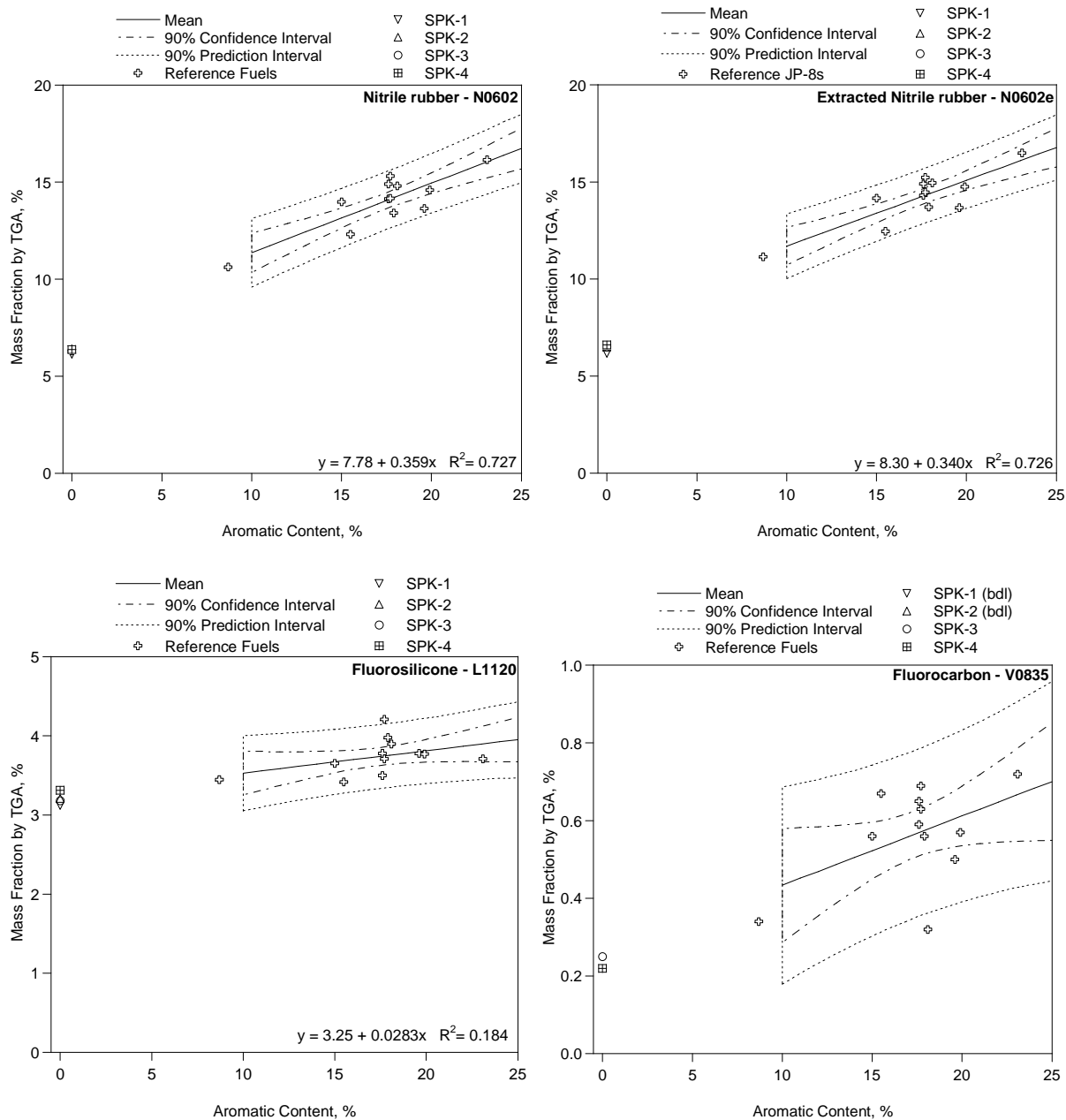


Figure 3-7. Summary of TGA results for the O-ring materials

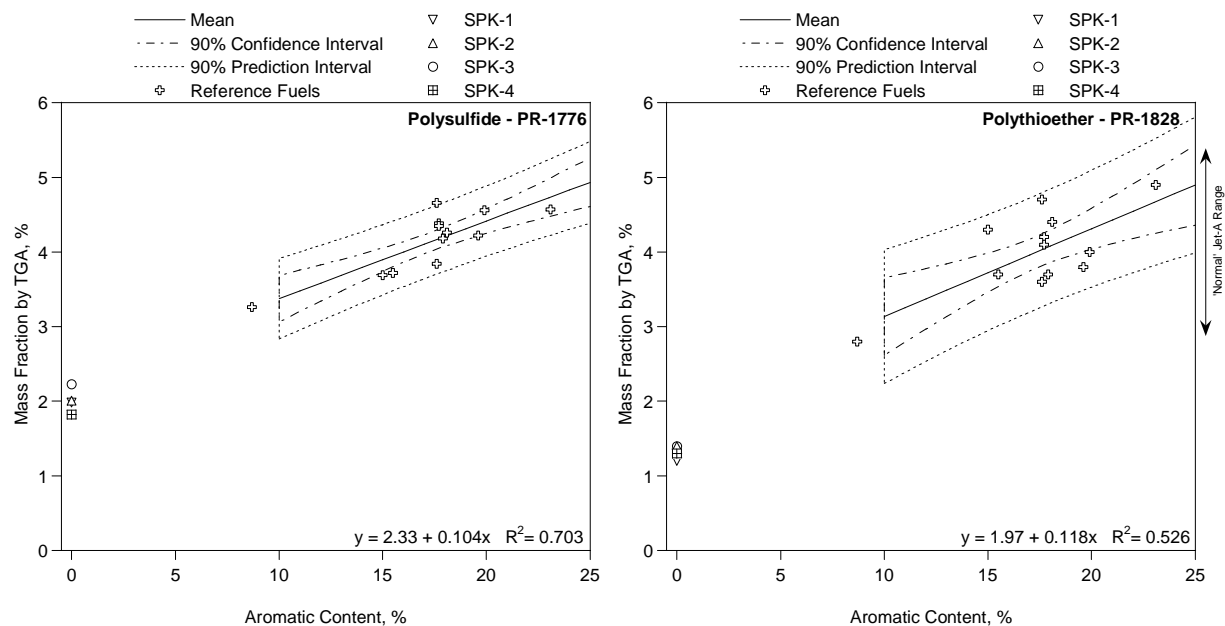


Figure 3-8. Summary of TGA results for the sealant materials

3.3 GC-MS Analysis of Absorbed Fuel

This discussion above illustrates that useful information may be obtained using a relatively simple method such as TGA to measure the mass fraction of fuel being absorbed by polymers aged in jet fuel. However, this technique has limited sensitivity (about 0.1% m/m) and may be challenged by interferences from semi-volatile components that cannot be clearly discriminated from fuel in the source weight loss data. By itself TGA also does not provide any information as to the composition of the absorbed fuel. However, this information may be obtained by analyzing the absorbed fuel using gas chromatography-mass spectrometry (GC-MS). Furthermore, comparing the analysis of the fuel absorbed with the fuel in which the sample was aged allows the relative solubility of the major class fractions and even individual fuel components in terms of their polymer-fuel partition coefficients (K_{pf}). This same data can be used to estimate the overall composition of the absorbed fuel which in turn reflects how each class fraction contributes to the observed volume swell.

Example GC-MS chromatograms for the fuel absorbed by the O-ring and sealant materials as well as the fuel in which they were aged are shown in Figure 3-9 to Figure 3-13. (Note that the coating and film materials did not absorb enough fuel to be analyzed by the method used here.) The average partition coefficients for the alkanes, alkyl benzenes (Alkyl Bz), naphthalene (Naph), and alkyl naphthalenes (Naphs) are summarized in Table 3-2. The estimated average composition of the fuel absorbed by each material is summarized in Table 3-3.

Overall, the chromatograms shown in Figure 3-9 to Figure 3-13 show that the fuel absorbed by each material is very complex and in most cases is as complex as the fuel itself. This illustrates

that the fuel as a whole participates in the volume swell process and not just the aromatics. Close examination shows that the aromatics are absorbed with a higher degree of selectivity as compared to the alkanes, but not to the exclusion of the alkanes. With respect to the alkanes, examining the chromatograms for the example SPK (SPK-2) illustrates how each material responds to the molar volume of the fuel components. Specifically, since the alkanes are non-polar and cannot participate in hydrogen bonds (see Table 1-1) the only mechanism of selectivity by the materials is molar volume. Specifically, each of the chromatographic traces for the SPK absorbed by the test materials shows some degree of selectivity towards the low molecular weight components (those on the left end of the chromatograms). This is most notable in the data for the fluorocarbon O-ring material (V0835 in Figure 3-11) which shows a high degree of selectivity towards the light end of the chromatogram.

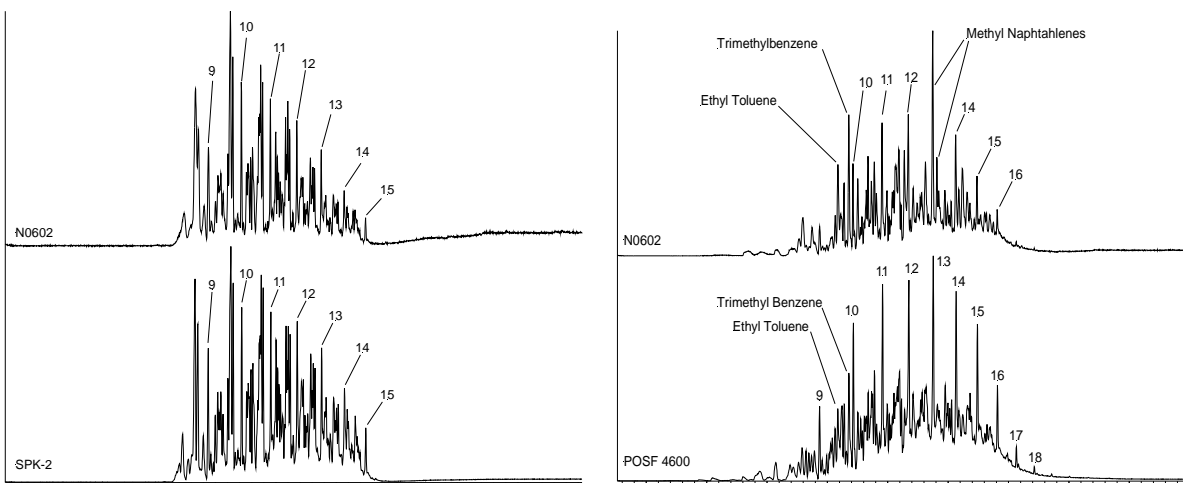


Figure 3-9. Example chromatograms comparing the fuel absorbed by the nitrile rubber (N0602) O-ring material (top) and the fuel in which they were aged (bottom). Note that normal alkanes are labeled with their carbon number

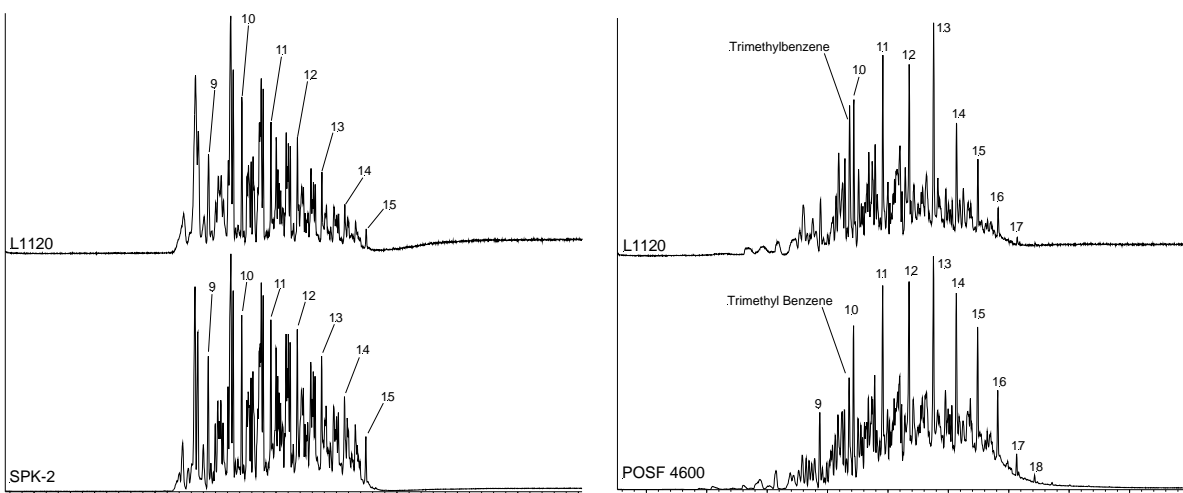


Figure 3-10. Example chromatograms comparing the fuel absorbed by the fluorosilicone (L1120) O-ring material (top) and the fuel in which they were aged (bottom). Note that normal alkanes are labeled with their carbon number

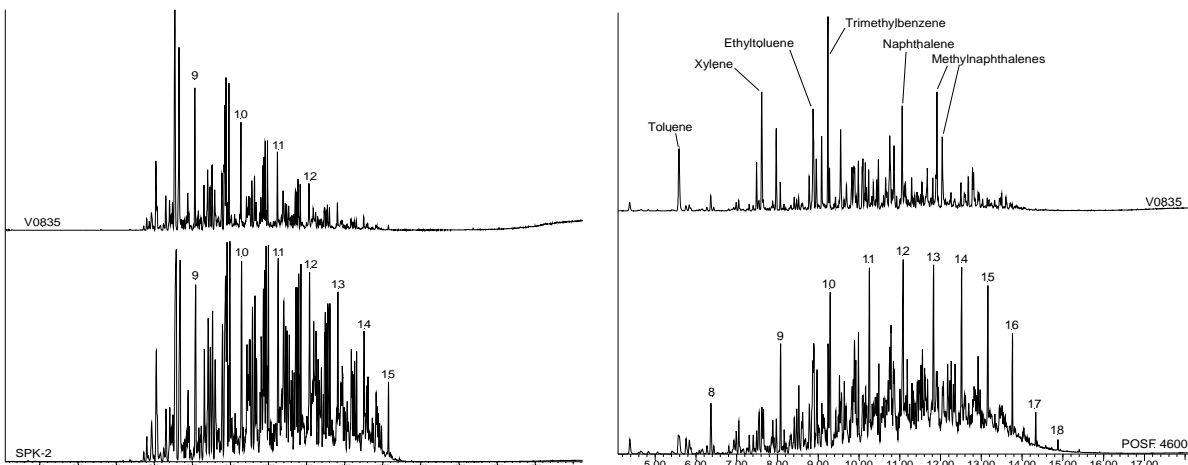


Figure 3-11. Example chromatograms comparing the fuel absorbed by the fluorocarbon (V0835) O-ring material (top) and the fuel in which they were aged (bottom). Note that normal alkanes are labeled with their carbon number

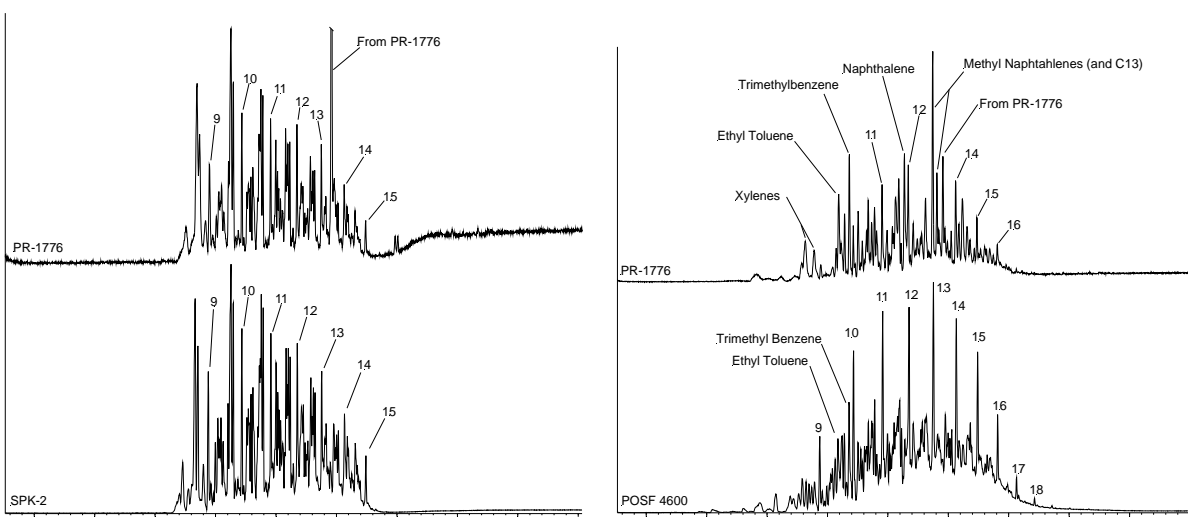


Figure 3-12. Example chromatograms comparing the fuel absorbed by the polysulfide (PR-1776) sealant material (top) and the fuel in which they were aged (bottom). Note that normal alkanes are labeled with their carbon number

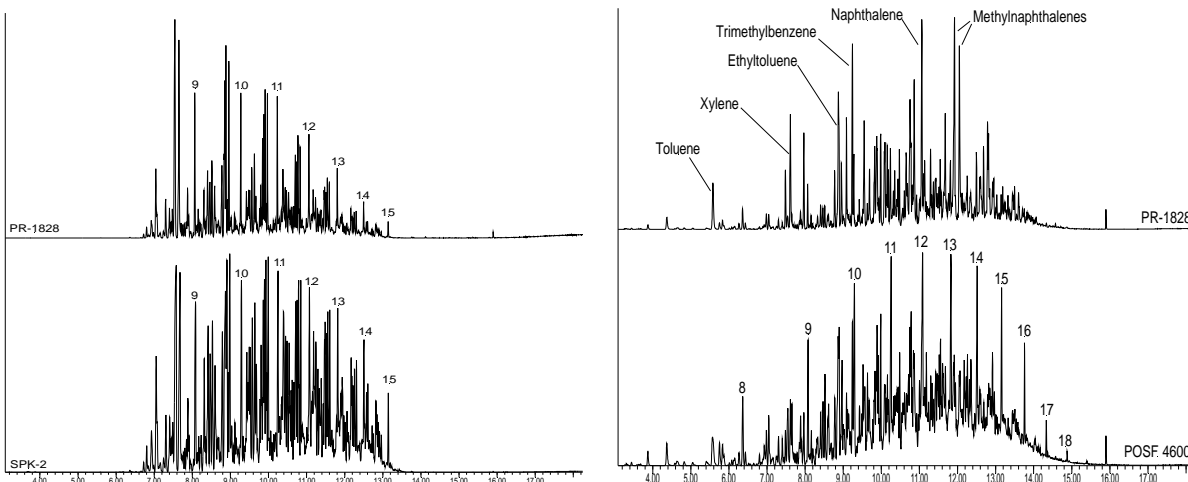


Figure 3-13. Example chromatograms comparing the fuel absorbed by the polythioether (PR-1828) material (top) and the fuel in which they were aged (bottom). Note that normal alkanes are labeled with their carbon number

Table 3-2 Average Polymer/Fuel Partition Coefficients

| Component | Material ID | SPK Alkanes | Averaged Jet-A | | | | Alkyl Bz/ Alkane |
|-----------|---|-------------|----------------|----------|-------|---------|---------------------|
| | | | Alkanes | Alkyl Bz | Naph* | Naphs** | |
| O-rings | N0602 | 0.103 | 0.126 | 0.422 | 1.065 | 0.705 | 3.35 |
| | L1120 | 0.077 | 0.059 | 0.121 | 0.220 | 0.131 | 2.05 |
| | V0835 | 0.011 | 0.011 | 0.085 | 0.230 | 0.124 | 7.73 |
| Sealants | PR-1776 | 0.035 | 0.044 | 0.181 | 0.796 | 0.389 | 4.11 |
| | PR-1828 | 0.027 | 0.029 | 0.189 | 0.775 | 0.419 | 6.52 |
| All | Average ratio of Kpf(Alkyl Benzenes)/Kpf(Alkanes) | | | | | | 4.75 |

*Naph = Naphthalene

**Naphs = Alkyl Naphthalenes

Table 3-3 Estimated Average Composition of Absorbed Fuel

| Component | Material ID | Alkanes | Alkyl Bz | Naphs |
|-----------|---------------|---------|----------|-------|
| O-rings | N0602 | 58.1% | 37.9% | 4.9% |
| | L1120 | 69.8% | 28.2% | 2.4% |
| | V0835 | 38.1% | 56.1% | 6.9% |
| Sealants | PR-1776 | 52.3% | 42.1% | 6.8% |
| | PR-1828 | 41.4% | 51.6% | 8.5% |
| All | Average | 51.9% | 43.2% | 5.9% |
| | | | | |
| Fuel | Average Jet-A | 82.6% | 16.3% | 1.1% |

With respect to the aromatics, the partition coefficients shown in Table 3-2 shows that the solubility of the class fractions examined here increase as alkanes, alkyl benzenes, alkyl naphthalenes, and naphthalene. This order of selectivity is a consequence of the molecular

characteristics of these fuel components. As shown in Table 1-1 the alkanes are the largest molecules present in jet fuel and exhibit only dispersive (non-polar) intermolecular bonding. The alkyl benzenes are smaller and exhibit some polarity and hydrogen bonding. The alkyl naphthalenes can exhibit polarity and hydrogen bonding that is somewhat higher than the alkyl benzenes, and naphthalene (one of the smallest aromatics found in jet fuel, and limited to 3%) exhibits the highest level of hydrogen bonding.

The highest degree of selectivity towards the aromatics versus the alkanes was found for fluorocarbon O-ring material (V0835) as shown in Table 3-2. Specifically, this Table shows that the solubility of the aromatics from Jet-A was an average of 7.73 times higher than the alkanes for this material. However, the absolute value of the solubility as reflected by the Kpf values is quite low so that this selectivity does not result in significant overall volume swell. The lowest selectivity was found for the fluorosilicone O-ring material (L1120) with the solubility of the aromatics from Jet-A being an average of 2.05 times higher than the alkanes. This is consistent with the volume swell results which showed a very weak correlation between the volume swell and the aromatic content of the fuel for this material. On-average, as shown in Table 3-2, it was found that aromatics from Jet-A were 4.75 times more soluble than the alkanes in the O-ring and sealant materials used here. However, as shown in Table 3-3, the alkanes are estimated to contribute approximately half of the volume swell to these materials. This is a consequence of the fact that while the alkanes are less soluble than the aromatics, they make up the majority of the fuel. Furthermore, based on the analysis described above, as the alkane distribution shifts to smaller and lighter molecules their influence on volume swell increases, and vice versa. This emphasizes the importance of considering the composition of the fuel as a whole and not focusing in on one particular class fraction of the fuel.

3.4 Volume Swell of 50% SPK/Jet-A Fuel Blends

At the time this study was proposed, our consideration was focused on fuels with low aromatic content (approximately 8%). The purpose of this task was to examine the volume swell of the test materials in fuels consisting of 50% blends of SPK-1 and the reference Jet-As and to examine the overlap between the 90% prediction intervals of the blends and reference fuels. This would include observing the overlap of the overall population of blends without regard to the aromatic content of the blend and the estimated volume swell for 50% SPK-1 blends with 8% aromatics.

The volume swell results for this study are summarized in Table 3-4 and in Figure 3-14 through Figure 3-17. These results show that amongst the test materials used here only the nitrile rubber O-ring material and the two sealant materials show any significant potential for exhibiting a volume swell character that is lower than the predicted range for Jet-A fuels used in this study when blended with 50% SPK-1 regardless of the aromatic content. When the aromatic content is restricted to 8%, only nitrile rubber and the polythioether sealant show the potential to exhibit volume swell that is lower than the predicted range for Jet-A used in this study. For example, for the as-received nitrile rubber the overall overlap in the 90% prediction intervals between the 50% SPK/Jet-A fuel blends and the reference Jet-As were found to be 44%, and at the value of 8%

aromatics the overlap as 23%. This suggests that if SPK-1 was arbitrarily blended at 50% with any Jet-A there is a 44% chance that the volume swell of that fuel would be within the Jet-A range as predicted by the reference fuels used here. Furthermore, if the 50% fuel blend contained 8% aromatics, then there is a 23% chance that the volume swell of that fuel would be within the Jet-A range as predicted by the reference fuels used here. It is very important to note that this is not a statistical prediction of success or failure, but merely a statistical prediction as to whether the volume swell of a given blend would fall within the estimated behavior for Jet-A fuels used in this study.

Table 3-4 Overlap of the 90% Prediction Intervals for 50% SPK/Jet-A Fuel Blends And 50% SPK/Jet-A Fuel Blends with 8% Aromatic Content

| Component | Sample ID | 50% SPK | 50% SPK 8% Aro. |
|------------------|------------------|----------------|----------------------------|
| O-Rings | N0602 | 44% | 23% |
| | N0602e | 51% | 34% |
| | L1120 | 100% | 100% |
| | V0835 | 100% | 100% |
| Sealants | PR 1776 | 88% | 100% |
| | PR 1828 | 57% | 56% |
| Coatings | BMS 10-20 | 100% | 100% |
| | BMS 10-123 | 96% | 100% |
| Films | Nylon | 80% | 100% |
| | Kapton | 100% | 100% |

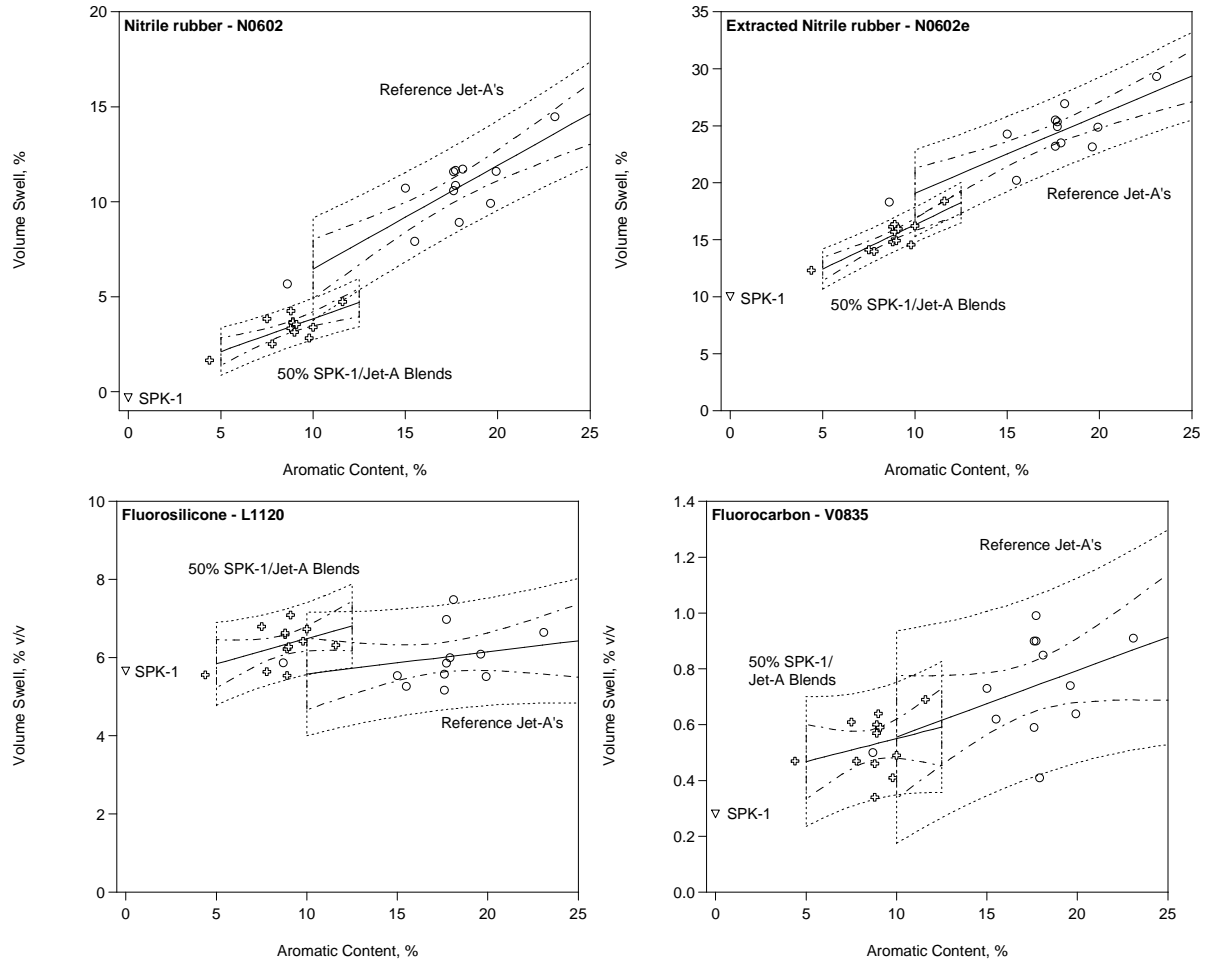


Figure 3-14. The volume swell of the O-ring materials after 40 hours at room temperature in the neat reference Jet-A's and 50% SPK-/Jet-A blends.

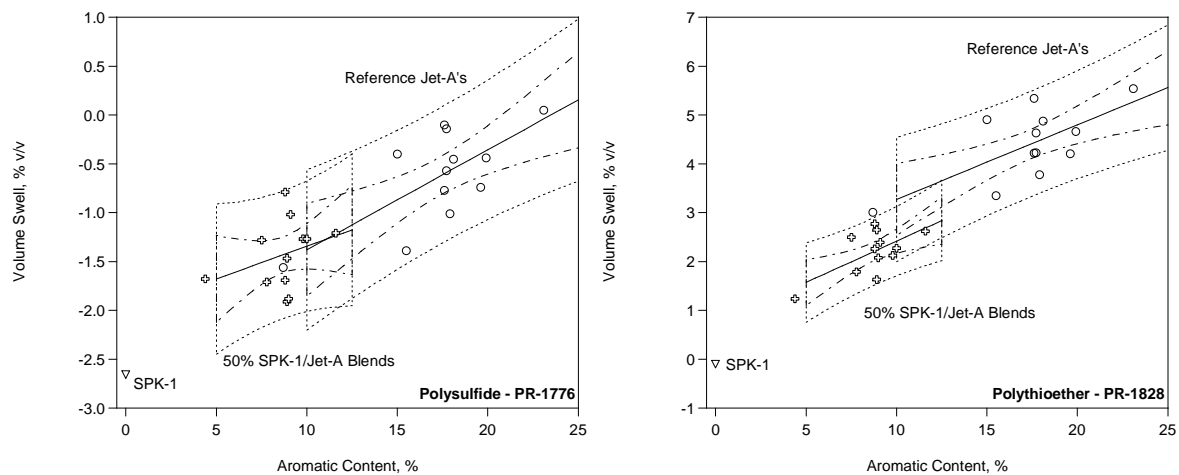


Figure 3-15. The volume swell of the sealant materials after 40 hours at room temperature in the neat reference Jet-A's and 50% SPK-/Jet-A blends

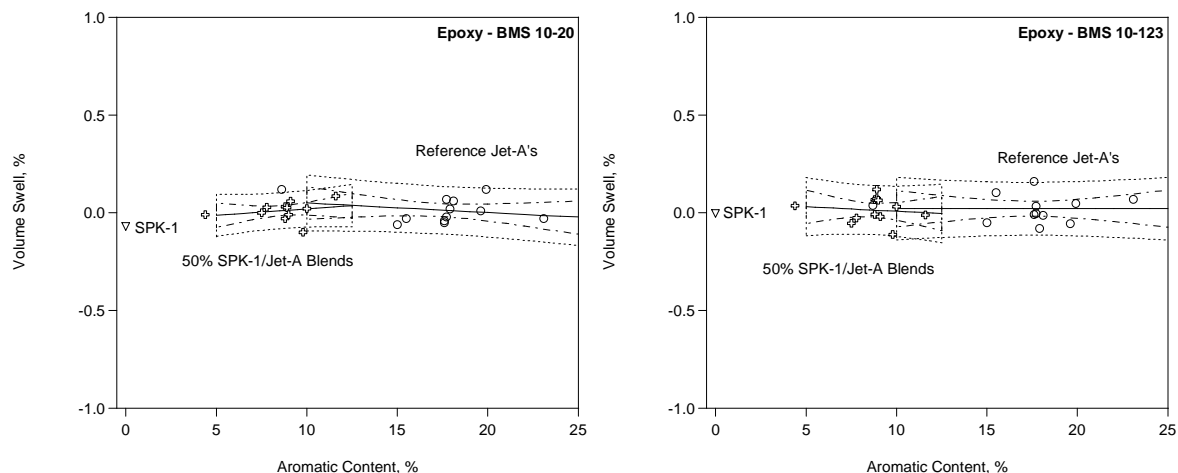


Figure 3-16. The volume swell of the coating materials after 40 hours at room temperature in the neat reference Jet-A's and 50% SPK-/Jet-A blends

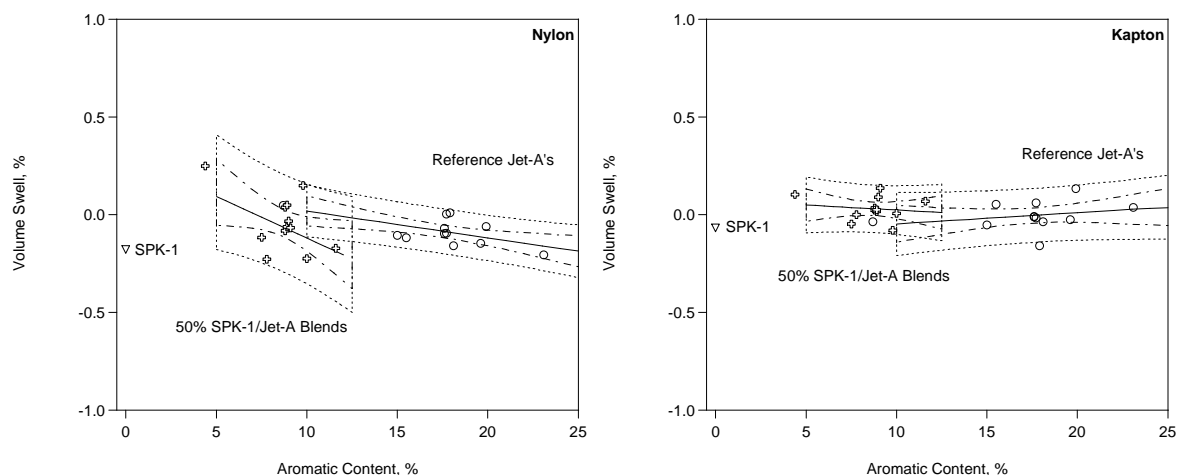


Figure 3-17. The volume swell of the film materials after 40 hours at room temperature in the neat reference Jet-A's and 50% SPK-/Jet-A blends

3.5 The Behavior of SPK Blended with Selected Aromatics

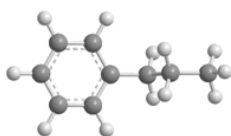
The analysis of the fuel absorbed by each of the test materials is very informative with regard to the activity of the major class fractions that naturally occur in jet fuel. However, it is very challenging to isolate the activity of individual fuel components due to the complexity of the fuel and the fact that individual components are typically present at very low concentrations. To evaluate the activity of specific types of aromatics a set of aromatics was selected as listed in Table 3-5 and shown in Figure 3-18. These aromatics were selected in an effort to isolate the relative roles of molar volume (propyl-, butyl-, and pentylbenzene), polarity (1,3,5-, 1,2,4-, and 1,2,3-trimethylbenzene), and hydrogen bonding (tetrahydronaphthalene and naphthalene). Furthermore, indan was selected as a component that is common in jet fuel and is structurally similar to tetrahydronaphthalene. Methylindene was selected as an olefinic form of indan (indene was preferred, but proved to be unstable). The treatment level was set at 8% in SPK-1 to

determine if this level was sufficient to raise the volume swell of each material into the range for Jet-A fuels in this study. Note that 3% was selected for naphthalene as this is the maximum level allowed in jet fuel and the same level was selected for methylindene. The relative activity of each aromatic was measured in terms of the specific swell. Supporting data was obtained in the form of the polymer-fuel partition coefficients for each of the aromatics. This provided a measure of the solubility of each individual aromatic whereas the volume swell was a measure of the overall absorption of fuel by each material.

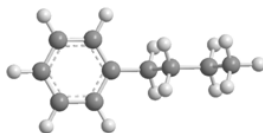
Table 3-5 Aromatics Used in this Study

| Characteristic | ID | Aromatic | Conc. %v/v | HSPs, MPa ^{1/2} | | | Density gm/mL | MV mL/mol |
|------------------|----|-------------------------|---------------|--------------------------|-------|--------|------------------|--------------|
| | | | | Disp. | Polar | H-Bond | | |
| Molar Volume | 1 | Propylbenzene* | 8% | 17.6 | 0.2 | 1.3 | 0.86 | 139 |
| | 2 | Butylbenzene | 8% | 17.4 | 0.1 | 1.1 | 0.86 | 157 |
| | 3 | Pentylbenzene* | 8% | 17.1 | 0.0 | 0.8 | 0.86 | 173 |
| Polarity | 4 | 1,3,5-Trimethylbenzene | 8% | 18.0 | 0.0 | 0.6 | 0.86 | 140 |
| | 5 | 1,2,4-Trimethylbenzene | 8% | 17.8 | 0.4 | 1.0 | 0.88 | 137 |
| | 6 | 1,2,3-Trimethylbenzene* | 8% | 17.6 | 0.8 | 1.4 | 0.89 | 134 |
| Hydrogen Bonding | 7 | Tetrahydronaphthalene | 8% | 19.6 | 2.0 | 2.9 | 0.97 | 136 |
| | 8 | Naphthalene | 3% | 19.2 | 2.0 | 5.9 | 1.03 | 112 |
| Other | 9 | Indan* | 8% | 17.8 | 0.6 | 2.1 | 0.97 | 123 |
| | 10 | Methylindene* | 3% | 20.1 | 1.0 | 7.2 | 0.97 | 134 |

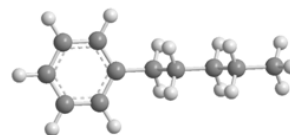
*HSPs estimated from structural analogs.



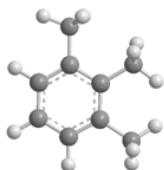
Propylbenzene



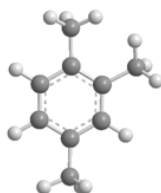
Butylbenzene



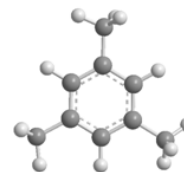
Pentylbenzene



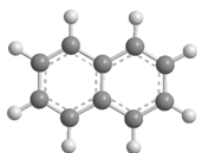
1,2,3-Trimethylbenzene



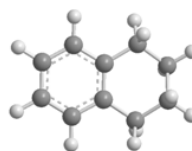
1,2,4-Trimethylbenzene



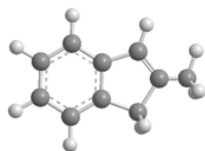
1,3,5-Trimethylbenzene



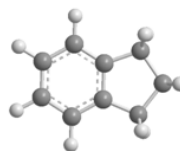
Naphthalene



Tetrahydronaphthalene



2-Methylindene



Indan

Figure 3-18. Molecular structures of the aromatic selected for this study.

The volume swell results are summarized in Table 3-6 (O-rings and sealants) and Table 3-7 (coatings and films). These tables also list the limits of the 90% prediction intervals for the reference Jet-As and the volume swell of the neat SPK-1. Values that are within the Jet-A range as predicted by the 90% prediction intervals are listed in bold type. Note that the volume swell of the fluorosilicone and fluorocarbon O-rings as well as all of the coatings and films aged in SPK-1 were all within the Jet-A range and no additional aromatics are needed for these materials based on this criterion. Of the remaining materials, the volume swell of the polysulfide sealant (PR-1776) in SPK-1 was near the lower bound of the 90% prediction interval and all of the aromatics used here promoted the volume swell of this material into the Jet-A range at their respective treatment levels. Similar results were found for the polythioether sealant (PR-1828) where most of the aromatics successfully promoted the volume swell of this materials into the Jet-A range with the exception of the two largest aromatics (butylbenzene and pentylbenzene) and the least polar aromatic (1,3,5-trimethylbenzene), in their respective series. The most impacted material was the nitrile rubber for which relatively few of the aromatics promoted sufficient volume swell to reach nominal swell found in the Jet-A range.

Table 3-6 Summary of Volume Swell Results for the O-ring and Sealants aged in SPK-1 Blended with Selected Aromatics

| Characteristic | Aromatic | O-Rings* | | | | Sealants* | |
|----------------|------------------------|-------------|--------------|-------------|-------------|--------------|-------------|
| | | N0602 | N0602e | L1120 | V0835 | PR-1776 | PR-1828 |
| Jet-A Range | 90% PI Upper Limit | 17.4% | 33.2% | 8.0% | 1.3% | 1.0% | 6.8% |
| | 90% PI Lower Limit | 3.7% | 15.3% | 4.0% | 0.2% | -2.2% | 2.0% |
| Molar Volume | Propylbenzene | 2.4% | 14.5% | 7.5% | 0.9% | -1.4% | 2.1% |
| | Butylbenzene | 2.0% | 13.3% | 7.8% | 0.6% | -1.9% | 1.6% |
| | Pentylbenzene | 1.4% | 12.2% | 6.0% | 0.6% | -1.7% | 1.4% |
| Polarity | 1,3,5-Trimethylbenzene | 2.3% | 14.2% | 6.8% | 0.8% | -1.8% | 1.4% |
| | 1,2,4-Trimethylbenzene | 3.3% | 15.3% | 5.4% | 1.1% | -0.8% | 2.9% |
| | 1,2,3-Trimethylbenzene | 4.3% | 16.6% | 7.5% | 1.1% | -0.8% | 3.6% |
| H-Bonding | Tetrahydronaphthalene | 4.6% | 14.9% | 8.1% | 0.4% | -0.4% | 3.6% |
| | Naphthalene | 3.4% | 15.8% | 6.7% | 0.7% | -0.4% | 4.4% |
| Other | Indan | 4.1% | 15.3% | 6.5% | 1.0% | 0.3% | 4.8% |
| | Methylindene | 2.1% | 13.2% | 7.4% | 0.8% | -1.9% | 2.4% |
| SPK-1 | None | -0.3% | 10.0% | 5.7% | 0.3% | -2.7% | -0.1% |

***Bold** denotes volume swell that is within the predicted Jet-A range.

Table 3-7 Summary of Volume Swell Results for the Coatings and Films aged in SPK-1 Blended with Selected Aromatics

| Characteristic | Aromatic | Coatings* | | Films* | |
|----------------|------------------------|--------------|-------------|--------------|--------------|
| | | BMS 10-20 | BMS 10-123 | Nylon | Kapton |
| Jet-A Range | 90% PI Upper Limit | 0.2% | 0.2% | 0.2% | 0.2% |
| | 90% PI Lower Limit | -0.2% | -0.1% | -0.3% | -0.2% |
| Molar Volume | Propylbenzene | 0.0% | 0.0% | -0.2% | 0.1% |
| | Butylbenzene | 0.0% | 0.0% | -0.1% | 0.1% |
| | Pentylbenzene | 0.0% | 0.0% | -0.2% | -0.1% |
| Polarity | 1,3,5-Trimethylbenzene | 0.0% | 0.0% | -0.3% | -0.1% |
| | 1,2,4-Trimethylbenzene | 0.0% | 0.1% | -0.3% | 0.1% |
| | 1,2,3-Trimethylbenzene | 0.0% | 0.1% | -0.2% | 0.0% |
| H-Bonding | Tetrahydronaphthalene | 0.0% | 0.0% | -0.2% | -0.1% |
| | Naphthalene | 0.0% | 0.0% | -0.2% | 0.0% |
| Other | Indan | 0.2% | 0.0% | -0.3% | 0.0% |
| | Methylindene | -0.1% | 0.0% | -0.2% | -0.1% |
| SPK-1 | None | -0.1% | 0.0% | -0.2% | -0.1% |

***Bold** denotes volume swell that is within the predicted Jet-A range.

The activity of each aromatic as expressed by the specific swell is summarized in Table 3-8 (O-rings and sealants) and Table 3-9 (coatings and films). These tables also list the average specific swell of the reference Jet-As which reflects the average activity of the aromatics that naturally occur in jet fuel. Values for the specific swell of the SPK-1 blended with the selected aromatics that are equal to or greater than the average Jet-As (used in this study) are shown in bold type.

These results illustrate that with the exception of nitrile rubber, the activity of most of the aromatics was equal to or greater than the average of those that naturally occur in jet fuel.

Table 3-8 Summary of Specific Swell Results for the O-ring and Sealants aged in SPK-1 Blended with Selected Aromatics at 8% (unless noted as 3%)

| Characteristic | Aromatic | O-Rings* | | | | Sealants* | |
|----------------|------------------------|-------------|-------------|-------------|-------------|-------------|-------------|
| | | N0602 | N0602e | L1120 | V0835 | PR-1776 | PR-1828 |
| Average Jet-A | Naturally Occuring | 0.55 | 0.69 | 0.06 | 0.02 | 0.10 | 0.15 |
| Molar Volume | Propylbenzene | 0.34 | 0.57 | 0.26 | 0.08 | 0.16 | 0.28 |
| | Butylbenzene | 0.29 | 0.41 | 0.19 | 0.04 | 0.10 | 0.22 |
| | Pentylbenzene | 0.21 | 0.28 | 0.06 | 0.03 | 0.12 | 0.19 |
| Polarity | 1,3,5-Trimethylbenzene | 0.33 | 0.53 | 0.08 | 0.07 | 0.10 | 0.19 |
| | 1,2,4-Trimethylbenzene | 0.45 | 0.66 | 0.04 | 0.10 | 0.24 | 0.38 |
| | 1,2,3-Trimethylbenzene | 0.57 | 0.82 | 0.16 | 0.10 | 0.24 | 0.46 |
| H-Bonding | Tetrahydronaphthalene | 0.61 | 0.61 | 0.12 | 0.01 | 0.28 | 0.46 |
| | Naphthalene (3%) | 1.22 | 1.92 | 0.29 | 0.15 | 0.74 | 1.51 |
| Other | Indan | 0.55 | 0.66 | 0.06 | 0.09 | 0.36 | 0.61 |
| | Methylindene (3%) | 0.81 | 1.07 | 0.61 | 0.18 | 0.27 | 0.84 |

***Bold** denotes specific swell that is equal to or greater than the average measured for Jet-A.

Table 3-9 Summary of Specific Swell Results for the Coatings and Films aged in SPK-1 Blended with Selected Aromatics

| Characteristic | Aromatic | Coatings* | | Films* | |
|----------------|------------------------|-------------|-------------|--------------|--------------|
| | | BMS 10-20 | BMS 10-123 | Nylon | Kapton |
| Average Jet-A | Naturally Occuring | 0.00 | 0.00 | -0.01 | 0.01 |
| Molar Volume | Propylbenzene | 0.01 | 0.01 | -0.01 | 0.02 |
| | Butylbenzene | 0.01 | 0.00 | 0.01 | 0.02 |
| | Pentylbenzene | 0.01 | 0.00 | 0.00 | -0.01 |
| Polarity | 1,3,5-Trimethylbenzene | 0.01 | 0.00 | -0.01 | -0.01 |
| | 1,2,4-Trimethylbenzene | 0.01 | 0.01 | -0.01 | 0.02 |
| | 1,2,3-Trimethylbenzene | 0.01 | 0.01 | 0.00 | 0.01 |
| H-Bonding | Tetrahydronaphthalene | 0.00 | 0.00 | -0.01 | 0.00 |
| | Naphthalene | 0.02 | -0.01 | -0.02 | 0.01 |
| Other | Indan | 0.03 | 0.00 | -0.01 | 0.01 |
| | Methylindene | -0.01 | 0.00 | 0.00 | -0.01 |

***Bold** denotes specific swell that is equal to or greater than the average measured for Jet-A.

The trends in the activity of the selected aromatics are illustrated in Figure 3-19 through Figure 3-21 for molar volume, polarity, and hydrogen bonding, respectively. These show that for the soft materials (the O-rings and sealants) the volume swell tends to increase as the molar volume of the aromatic decreases, and as the polarity and hydrogen bonding increases. Amongst these three factors (molar volume, polarity, hydrogen bonding) molar volume had the least influence on the volume swell followed by polarity and hydrogen bonding. Furthermore, the influence of hydrogen bonding tended to be significantly higher than that of polarity. For the hard materials (coatings and films) the aromatics had little effect. This suggests that materials that are inert in Jet-A will also be inert in SPKs and SPKs blended with aromatics being used as swelling promoters.

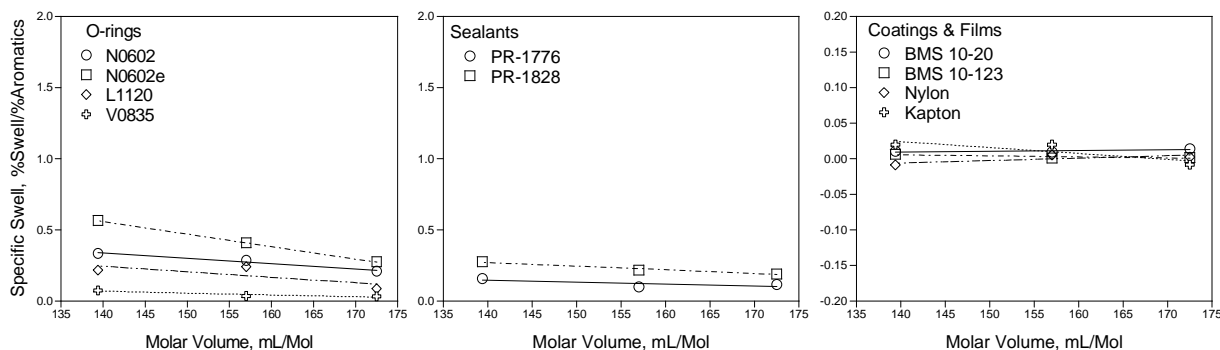


Figure 3-19. Specific swell as a function of the molar volume of the aromatic blended with SPK-1

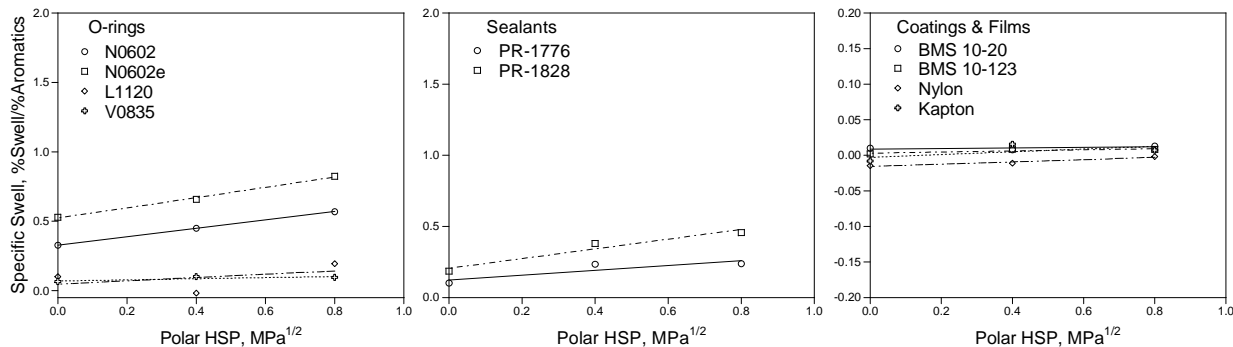


Figure 3-20. Specific swell as a function of the polar HSP of the aromatic blended with SPK-1

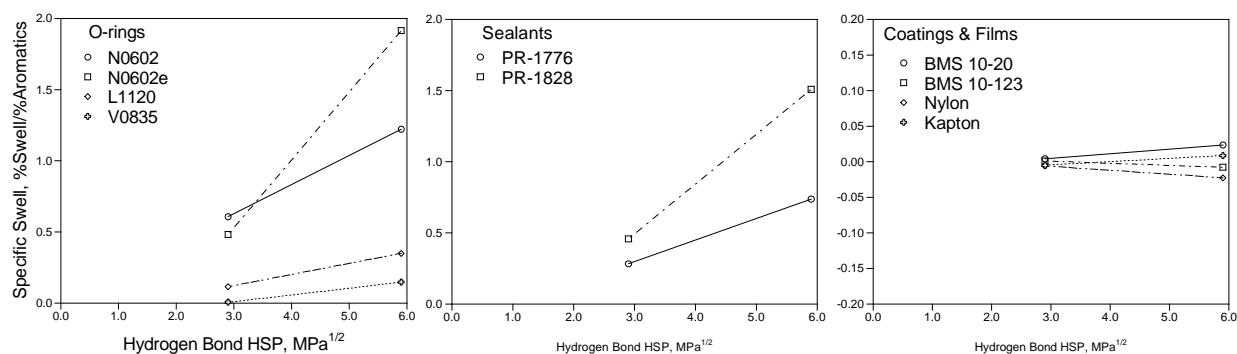


Figure 3-21. Specific swell as a function of the hydrogen bond HSP of the aromatic blended with SPK-1

The relative solubility of the specific aromatics in the O-rings and sealants are summarized in Table 3-10 and Figure 3-22 through Figure 3-24 for molar volume, polarity, and hydrogen bonding, respectively. (Note that the coatings and films did not absorb enough fuel to be analyzed by the methods used here.) The overall results are similar to that found for the volume swell, though more subtle. Specifically, solubility of the specific aromatics tended to increase as the molar volume of the aromatic decreases, and as the polarity and hydrogen bonding increases. Furthermore, over the range used in this study, the relative influence increased as molar volume, polarity, and hydrogen bonding.

Table 3-10 Summary of Partition Coefficient Results for the O-ring and Sealants aged in SPK-1 Blended with Selected Aromatics

| Characteristic | Aromatic | O-Rings* | | | Sealants* | |
|----------------|------------------------|-------------|-------------|-------------|-------------|-------------|
| | | N0602 | L1120 | V0835 | PR-1776 | PR-1828 |
| Average Jet-A | Naturally Occuring | 0.42 | 0.12 | 0.09 | 0.18 | 0.19 |
| Molar Volume | Propylbenzene | 0.44 | 0.17 | 0.08 | 0.21 | 0.24 |
| | Butylbenzene | 0.49 | 0.18 | 0.05 | 0.20 | 0.23 |
| | Pentylbenzene | 0.46 | 0.15 | 0.04 | 0.17 | 0.20 |
| Polarity | 1,3,5-Trimethylbenzene | 0.45 | 0.12 | 0.10 | 0.17 | 0.20 |
| | 1,2,4-Trimethylbenzene | 0.50 | 0.17 | 0.12 | 0.23 | 0.24 |
| | 1,2,3-Trimethylbenzene | 0.52 | 0.15 | 0.10 | 0.24 | 0.29 |
| H-Bonding | Tetrahydronaphthalene | 0.60 | 0.14 | 0.07 | 0.30 | 0.34 |
| | Naphthalene | 1.20 | 0.23 | 0.19 | 0.72 | 0.91 |
| Other | Indan | 0.48 | 0.14 | 0.10 | 0.31 | 0.20 |
| | Methylindene | 0.82 | 0.21 | 0.18 | 0.41 | 0.54 |

***Bold** denotes partition coefficients that are equal to or greater than the average measured for Jet-A.

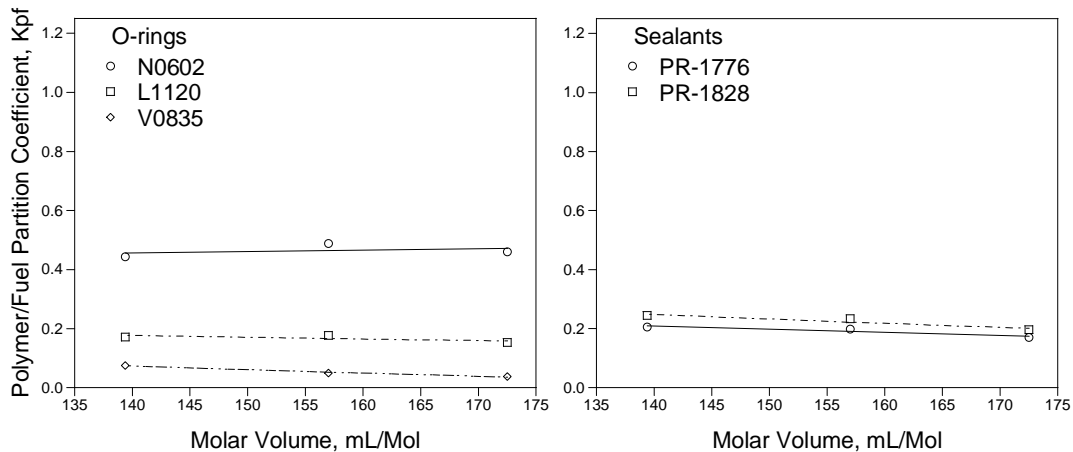


Figure 3-22. Polymer-fuel partition coefficients as a function of the molar volume of the aromatic blended with SPK-1

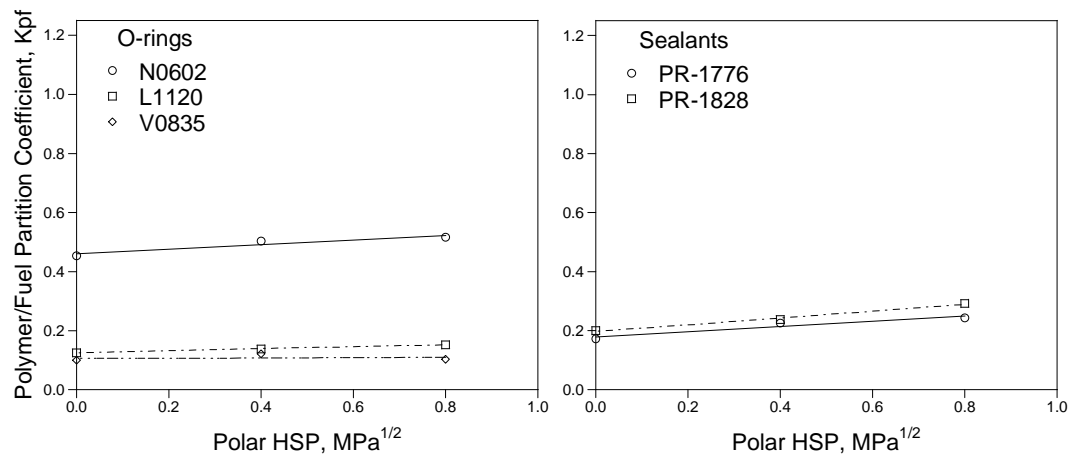


Figure 3-23. Polymer-fuel partition coefficients as a function of the polar HSP of the aromatic blended with SPK-1

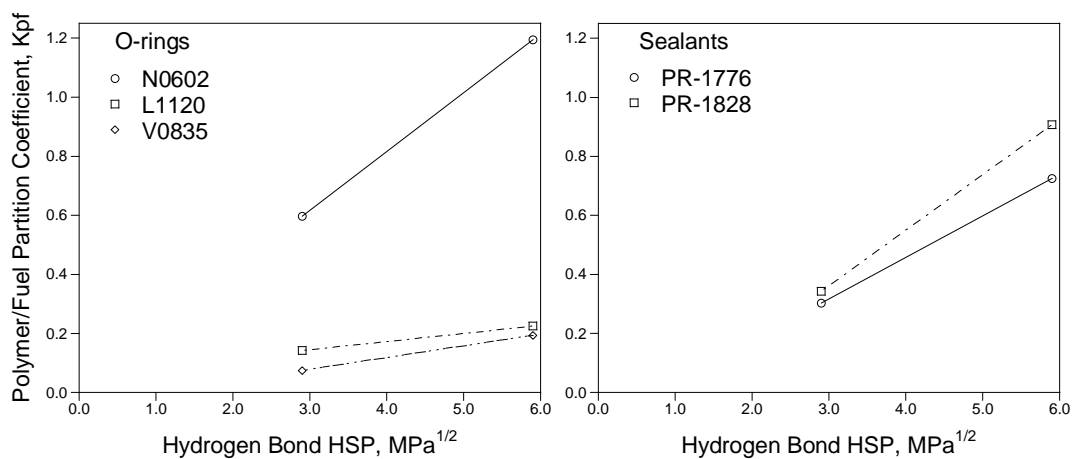


Figure 3-24. Polymer-fuel partition coefficients as a function of the hydrogen bond HSP of the aromatic blended with SPK-1

With respect to the indan and methyindene, for the materials that showed the greatest influence of the aromatic content of the fuel (the nitrile rubber and the polysulfide and polythioether sealants) the activity of the indan was slightly higher than tetrahydronaphthalene and the activity of the methyindene was intermediate between that of the tetrahydronaphthalene and naphthalene (see Table 3-8). This suggests that these two aromatics could serve as effective swelling promoters, though their performance is not exceptional.

4 Technical Summary

A study has been completed to examine the overall effect of SPK and SPK fuel blends on non-metallic materials used in commercial aircraft fuel systems. The primary measure of performance was the volume swell of dry source materials immersed in fuel for 40 hours at room temperature. Supporting data was obtained in the form of an analysis of the fuel absorbed by each test material using either thermogravimetric analysis as well as thermal desorption gas chromatography-mass spectrometry. The volume swell and fuel absorbed using a set of 12 Jet-As and 4 SPKs were used as the primary basis for comparison. The Jet-As were selected to span a broad range of aromatics (from 8.7% to 23.1%) while the SPKs were selected from a variety of sources, though they were processed into 4 very similar fuels with 0% aromatics. To evaluate the relative importance of the molecular structure of fuel components in general, and aromatics in particular, the activity of 10 aromatics selected to emphasize the relative roles of molar volume, polarity, and hydrogen bonding were measured and compared with the reference Jet-As. Furthermore, data was obtained on a set of fuels consisting of 50% SPK/Jet-A fuel blends to assess the performance of these fuels regardless of their aromatic content as well as those blends with 8% aromatics.

The overall response to the aromatic content of the fuel was found to be very material-dependent with the greatest effect being shown by a nitrile rubber O-ring material and a polythioether and -polysulfide sealant. A fluorocarbon O-ring material was found to be relatively inert while two epoxy coatings and a nylon and a Kapton® film were found to be essentially inert in all of the test fuels. A fluorosilicone O-ring material was found to show moderate volume swell behavior, however the volume swell of this material was a very weak function of the aromatic content. Although the volume swell of the test materials tended to increase with the aromatic of the fuel, only the nitrile rubber O-ring and polythioether and polysulfide sealant materials showed a volume swell character in the SPKs that was lower than the range predicted for Jet-A based on the reference fuels used here and only the nitrile rubber proved to be the most sensitive to aromatic content. ***It is very important to note that this is not a statistical prediction of success or failure, but merely a statistical prediction as to whether the volume swell of a given blend would fall within the predicted 'normal' range for Jet-A.*** Based on recent testing (and ASTM D7566-11 approval of a minimum of 8% aromatics content) of up to 50% SPK blends, it is believed that fuel system materials can perform their intended functions when using fuel which provides volume swell that might be lower than present in-service conditions. Beyond these recent approvals, more complete operational and engineering data of low aromatic fuels will likely be needed to determine how far outside the statistical bounds our present day experience can be extended.

With respect to the influence of the molecular structure of the fuel; volume swell was found to increase as the molar volume of the fuel components decreases and as their polarity and hydrogen bonding increases. Amongst these three factors (molar volume, polarity, hydrogen bonding) molar volume had the least influence on the volume swell followed by polarity and hydrogen bonding. Furthermore, the influence of hydrogen bonding tended to be significantly higher than that of polarity. This suggests that the volume swell of jet fuel will increase as the boiling range skews towards lower temperatures (lower molecular weight) and as the overall

polarity and hydrogen bonding increases, and vice versa. Noting that the bulk of Jet-A and all of typical SPKs are paraffinic and therefore non-polar, the polarity and hydrogen bonding character of the fuel will be dominated by the aromatics. However, emphasizing that the bulk of the fuel is paraffinic, particularly as the aromatic content is lowered, the influence of the molecular weight distribution of the fuel must be considered. This emphasizes the importance of taking into account the composition of a fuel as a whole when considering how it interacts with non-metallic materials and not focusing on one class fraction of the fuel.

5 Appendices

5.1 Appendix A N0602 Nitrile Rubber O-Ring

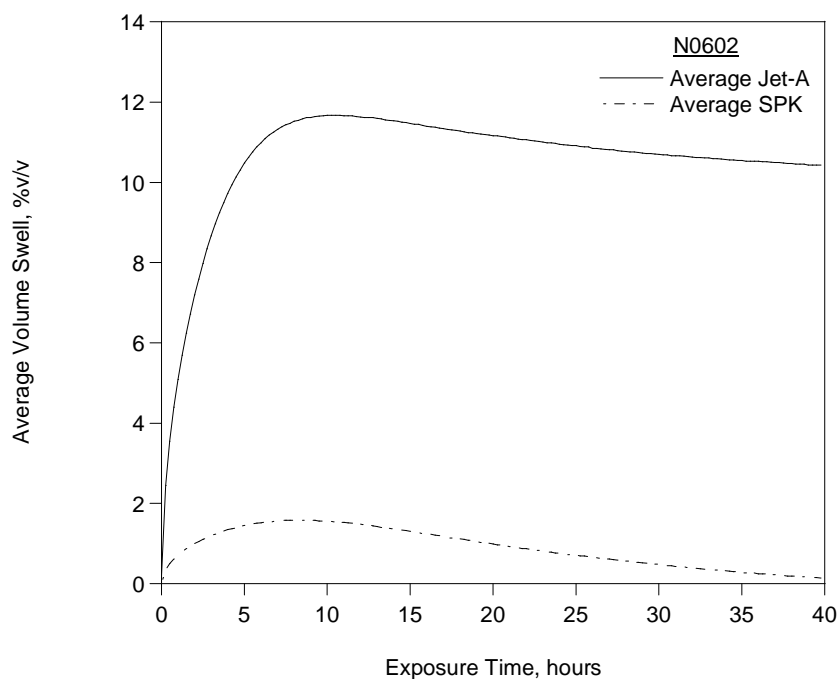


Figure A-1 Average volume swell as a function of time for N0602 at room temperature

Table A-1 Summary of Volume Swell and Mass Fraction of Fuel Absorbed by N0602

| Fuel ID | Aromatics D6379 | Naphs* D6379 | Volume Swell | Mass Fraction |
|---------|-----------------|--------------|--------------|---------------|
| SRI-1 | 8.7% | 0.2% | 5.7% | 11.2% |
| 4597 | 15.0% | 1.9% | 10.7% | 14.2% |
| 5245 | 15.5% | 0.2% | 7.9% | 12.5% |
| 3166 | 17.6% | 2.5% | 11.6% | 14.9% |
| 4598 | 17.6% | 1.4% | 10.6% | 14.3% |
| 4600 | 17.7% | 1.3% | 11.7% | 15.2% |
| 4658 | 17.7% | 1.3% | 10.9% | 14.5% |
| 4626 | 17.9% | 0.6% | 8.9% | 13.7% |
| 5661 | 18.1% | 0.6% | 11.7% | 14.9% |
| 4877 | 19.6% | 0.4% | 9.9% | 13.7% |
| 4599 | 19.9% | 1.4% | 11.6% | 14.7% |
| 3602 | 23.1% | 1.1% | 14.5% | 16.5% |
| SPK-1 | 0.0% | 0.0% | -0.3% | 6.2% |
| SPK-2 | 0.0% | 0.0% | 0.2% | 6.5% |
| SPK-3 | 0.0% | 0.0% | 0.1% | 6.5% |
| SPK-4 | 0.0% | 0.0% | 0.6% | 6.6% |

*Naphthalenes

Table A-2 Summary of Polymer-Fuel Partition Coefficients (Kpf) for N0602

| Fuel ID | Aromatics D6379 | Naphs* D6379 | Kpf | | | |
|---------|-----------------|--------------|---------|----------|-------|-------|
| | | | Alkanes | Alkyl Bz | Naph | Naphs |
| SRI-1 | 8.7% | 0.2% | 0.129 | 0.405 | ** | ** |
| 4597 | 15.0% | 1.9% | 0.142 | 0.520 | 1.294 | 0.946 |
| 5245 | 15.5% | 0.2% | 0.114 | 0.409 | ** | ** |
| 3166 | 17.6% | 2.5% | 0.135 | 0.450 | 1.196 | 0.829 |
| 4598 | 17.6% | 1.4% | 0.122 | 0.418 | 1.117 | 0.576 |
| 4600 | 17.7% | 1.3% | 0.108 | 0.334 | 0.864 | 0.609 |
| 4658 | 17.7% | 1.3% | 0.117 | 0.400 | 1.059 | 0.668 |
| 4626 | 17.9% | 0.6% | 0.128 | 0.430 | 1.090 | 0.701 |
| 5661 | 18.1% | 0.6% | 0.134 | 0.455 | 1.035 | 0.680 |
| 4877 | 19.6% | 0.4% | 0.116 | 0.407 | 0.970 | 0.640 |
| 4599 | 19.9% | 1.4% | 0.123 | 0.403 | 1.027 | 0.679 |
| 3602 | 23.1% | 1.1% | 0.143 | 0.434 | 1.000 | 0.720 |
| | | | | | | |
| Average | 17.4% | 1.2% | 0.126 | 0.422 | 1.065 | 0.705 |
| 90% CI | 1.6% | 0.3% | 0.006 | 0.023 | 0.062 | 0.057 |
| | | | | | | |
| SPK-1 | 0.0% | 0.0% | 0.096 | n.a. | n.a. | n.a. |
| SPK-2 | 0.0% | 0.0% | 0.098 | n.a. | n.a. | n.a. |
| SPK-3 | 0.0% | 0.0% | 0.114 | n.a. | n.a. | n.a. |
| SPK-4 | 0.0% | 0.0% | 0.103 | n.a. | n.a. | n.a. |

*Naphthalenes

**Concentration too low in the fuel for accurate quantification.

Table A-3 Estimated Composition of the Bulk and Absorbed Fuels

| Fuel ID | Bulk Fuel | | | Absorbed Fuel | | |
|---------|-----------|----------|--------|---------------|----------|--------|
| | Alkanes | Alkyl Bz | Naphs* | Alkanes | Alkyl Bz | Naphs* |
| SRI-1 | 91.3% | 8.5% | 0.2% | 86.6% | 13.4% | ** |
| 4597 | 85.0% | 13.1% | 1.9% | 58.3% | 33.0% | 8.7% |
| 5245 | 84.5% | 15.3% | 0.2% | 60.7% | 39.3% | ** |
| 3166 | 82.4% | 15.1% | 2.5% | 55.6% | 34.0% | 10.4% |
| 4598 | 82.4% | 16.2% | 1.4% | 57.0% | 38.4% | 4.6% |
| 4600 | 82.3% | 16.4% | 1.3% | 58.6% | 36.2% | 5.2% |
| 4658 | 82.3% | 16.4% | 1.3% | 56.6% | 38.4% | 5.1% |
| 4626 | 82.1% | 17.3% | 0.6% | 57.2% | 40.5% | 2.3% |
| 5661 | 81.9% | 17.5% | 0.6% | 56.7% | 41.2% | 2.1% |
| 4877 | 80.4% | 19.2% | 0.4% | 53.6% | 45.0% | 1.5% |
| 4599 | 80.1% | 18.5% | 1.4% | 53.9% | 40.9% | 5.2% |
| 3602 | 76.9% | 22.0% | 1.1% | 51.5% | 44.8% | 3.7% |
| | | | | | | |
| Average | 82.6% | 16.3% | 1.1% | 58.1% | 37.9% | 4.9% |
| 90% CI | 98.4% | 1.3% | 0.3% | 0.6% | 2.3% | 6.2% |
| | | | | | | |
| SPK-1 | 100.0% | 0.0% | 0.0% | 100.0% | 0.0% | 0.0% |
| SPK-2 | 100.0% | 0.0% | 0.0% | 100.0% | 0.0% | 0.0% |
| SPK-3 | 100.0% | 0.0% | 0.0% | 100.0% | 0.0% | 0.0% |
| SPK-4 | 100.0% | 0.0% | 0.0% | 100.0% | 0.0% | 0.0% |

*Naphthalenes **Concentration too low in the fuel for accurate quantification.

5.2 Appendix B N0602e Extracted Nitrile Rubber O-Ring

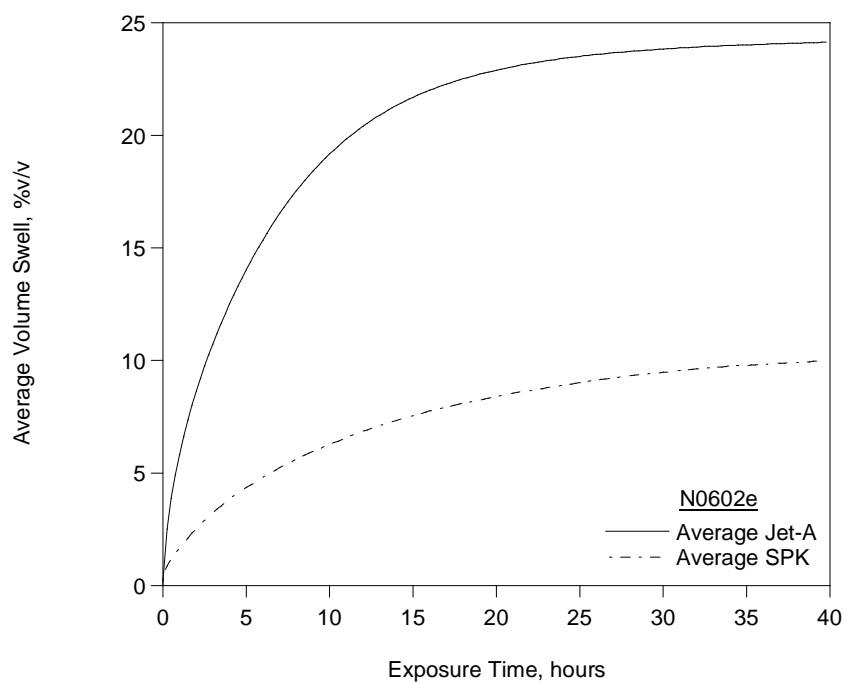


Figure B-1 Average volume swell as a function of time for N0602e at room temperature

Table B-1 Summary of Volume Swell and Mass Fraction of Fuel Absorbed by N0602e

| Fuel ID | Aromatics D6379 | Naphs* D6379 | Volume Swell | Mass Fraction |
|---------|-----------------|--------------|--------------|---------------|
| SRI-1 | 8.7% | 0.2% | 18.3% | 10.6% |
| 4597 | 15.0% | 1.9% | 24.3% | 14.0% |
| 5245 | 15.5% | 0.2% | 20.2% | 12.3% |
| 3166 | 17.6% | 2.5% | 25.5% | 14.9% |
| 4598 | 17.6% | 1.4% | 23.2% | 14.1% |
| 4600 | 17.7% | 1.3% | 25.4% | 15.3% |
| 4658 | 17.7% | 1.3% | 25.0% | 14.2% |
| 4626 | 17.9% | 0.6% | 23.5% | 13.4% |
| 5661 | 18.1% | 0.6% | 26.9% | 14.8% |
| 4877 | 19.6% | 0.4% | 23.1% | 13.6% |
| 4599 | 19.9% | 1.4% | 24.9% | 14.6% |
| 3602 | 23.1% | 1.1% | 29.3% | 16.2% |
| SPK-1 | 0.0% | 0.0% | 10.0% | 6.1% |
| SPK-2 | 0.0% | 0.0% | 9.9% | 6.4% |
| SPK-3 | 0.0% | 0.0% | 10.2% | 6.3% |
| SPK-4 | 0.0% | 0.0% | 9.9% | 6.4% |

*Naphthalenes

5.3 Appendix C L1120 Fluorosilicone O-Ring

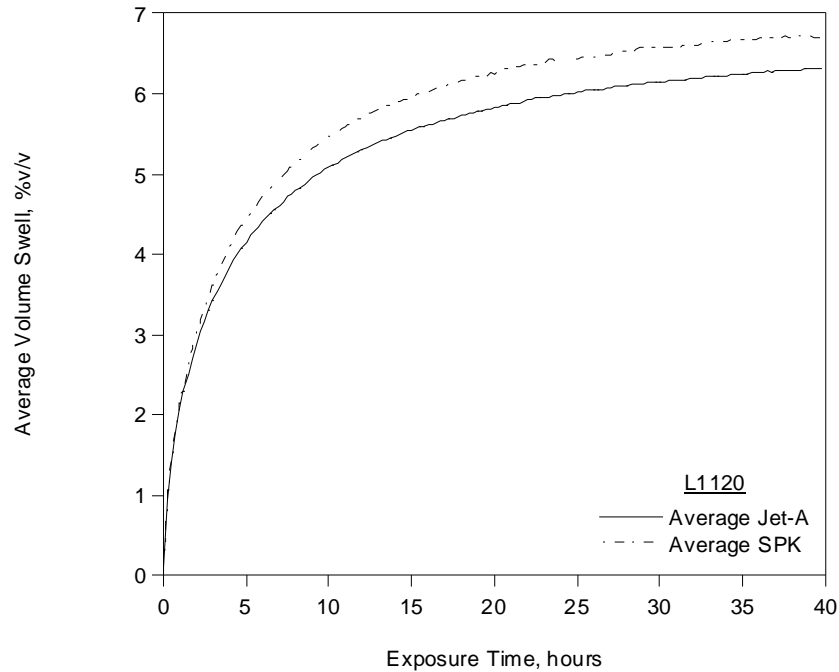


Figure C-1 Average volume swell as a function of time for L1120 at room temperature

Table C-1 Summary of Volume Swell and Mass Fraction of Fuel Absorbed by L1120

| Fuel ID | Aromatics D6379 | Naphs* D6379 | Volume Swell | Mass Fraction |
|---------|-----------------|--------------|--------------|---------------|
| SRI-1 | 8.7% | 0.2% | 5.9% | 3.5% |
| 4597 | 15.0% | 1.9% | 5.5% | 3.6% |
| 5245 | 15.5% | 0.2% | 5.3% | 3.4% |
| 3166 | 17.6% | 2.5% | 5.6% | 3.8% |
| 4598 | 17.6% | 1.4% | 5.2% | 3.5% |
| 4600 | 17.7% | 1.3% | 7.0% | 4.2% |
| 4658 | 17.7% | 1.3% | 5.9% | 3.7% |
| 4626 | 17.9% | 0.6% | 6.0% | 4.0% |
| 5661 | 18.1% | 0.6% | 7.5% | 3.9% |
| 4877 | 19.6% | 0.4% | 6.1% | 3.8% |
| 4599 | 19.9% | 1.4% | 5.5% | 3.8% |
| 3602 | 23.1% | 1.1% | 6.6% | 3.7% |
| SPK-1 | 0.0% | 0.0% | 5.7% | 3.1% |
| SPK-2 | 0.0% | 0.0% | 6.6% | 3.2% |
| SPK-3 | 0.0% | 0.0% | 6.6% | 3.2% |
| SPK-4 | 0.0% | 0.0% | 6.9% | 3.3% |

*Naphthalenes

Table C-2 Summary of Polymer-Fuel Partition Coefficients (Kpf) for L1120

| Fuel ID | Aromatics D6379 | Naphs* D6379 | Kpf | | | |
|---------|-----------------|--------------|---------|----------|-------|--------|
| | | | Alkanes | Alkyl Bz | Naph | Naphs* |
| SRI-1 | 8.7% | 0.2% | 0.068 | 0.112 | ** | ** |
| 4597 | 15.0% | 1.9% | 0.057 | 0.135 | 0.245 | 0.162 |
| 5245 | 15.5% | 0.2% | 0.059 | 0.123 | ** | ** |
| 3166 | 17.6% | 2.5% | 0.055 | 0.117 | 0.229 | 0.144 |
| 4598 | 17.6% | 1.4% | 0.045 | 0.097 | 0.193 | 0.092 |
| 4600 | 17.7% | 1.3% | 0.056 | 0.107 | 0.190 | 0.115 |
| 4658 | 17.7% | 1.3% | 0.059 | 0.123 | 0.233 | 0.131 |
| 4626 | 17.9% | 0.6% | 0.073 | 0.147 | 0.252 | 0.148 |
| 5661 | 18.1% | 0.6% | 0.065 | 0.136 | 0.225 | 0.138 |
| 4877 | 19.6% | 0.4% | 0.063 | 0.131 | 0.221 | 0.129 |
| 4599 | 19.9% | 1.4% | 0.062 | 0.125 | 0.229 | 0.132 |
| 3602 | 23.1% | 1.1% | 0.050 | 0.103 | 0.184 | 0.120 |
| Average | 18.2% | 1.2% | 0.059 | 0.121 | 0.220 | 0.131 |
| 90% CI | 1.1% | 0.3% | 0.004 | 0.008 | 0.012 | 0.010 |
| SPK-1 | 0.0% | 0.0% | 0.077 | n.C. | n.C. | n.C. |
| SPK-2 | 0.0% | 0.0% | 0.081 | n.C. | n.C. | n.C. |
| SPK-3 | 0.0% | 0.0% | 0.089 | n.C. | n.C. | n.C. |
| SPK-4 | 0.0% | 0.0% | 0.060 | n.C. | n.C. | n.C. |

*Naphthalenes

**Concentration too low in the fuel for accurate quantification.

Table C-3 Estimated Composition of the Bulk and Absorbed Fuels

| Fuel ID | Bulk Fuel | | | Absorbed Fuel | | |
|---------|-----------|----------|--------|---------------|----------|--------|
| | Alkanes | Alkyl Bz | Naphs* | Alkanes | Alkyl Bz | Naphs* |
| SRI-1 | 91.3% | 8.5% | 0.2% | 86.6% | 13.4% | ** |
| 4597 | 85.0% | 13.1% | 1.9% | 69.9% | 25.6% | 4.5% |
| 5245 | 84.5% | 15.3% | 0.2% | 72.5% | 27.5% | ** |
| 3166 | 82.4% | 15.1% | 2.5% | 67.9% | 26.6% | 5.4% |
| 4598 | 82.4% | 16.2% | 1.4% | 68.7% | 28.9% | 2.4% |
| 4600 | 82.3% | 16.4% | 1.3% | 70.6% | 27.1% | 2.3% |
| 4658 | 82.3% | 16.4% | 1.3% | 69.0% | 28.6% | 2.4% |
| 4626 | 82.1% | 17.3% | 0.6% | 69.6% | 29.4% | 1.0% |
| 5661 | 81.9% | 17.5% | 0.6% | 68.3% | 30.6% | 1.1% |
| 4877 | 80.4% | 19.2% | 0.4% | 66.3% | 33.0% | 0.7% |
| 4599 | 80.1% | 18.5% | 1.4% | 66.5% | 31.0% | 2.5% |
| 3602 | 76.9% | 22.0% | 1.1% | 61.4% | 36.5% | 2.1% |
| Average | 82.6% | 16.3% | 1.1% | 69.8% | 28.2% | 2.4% |
| 90% CI | 98.9% | 0.7% | 0.3% | 0.4% | 0.8% | 1.2% |
| SPK-1 | 100.0% | 0.0% | 0.0% | 100.0% | 0.0% | 0.0% |
| SPK-2 | 100.0% | 0.0% | 0.0% | 100.0% | 0.0% | 0.0% |
| SPK-3 | 100.0% | 0.0% | 0.0% | 100.0% | 0.0% | 0.0% |
| SPK-4 | 100.0% | 0.0% | 0.0% | 100.0% | 0.0% | 0.0% |

*Naphthalenes

**Concentration too low in the fuel for accurate quantification.

5.4 Appendix D V0835 Fluorocarbon O-ring

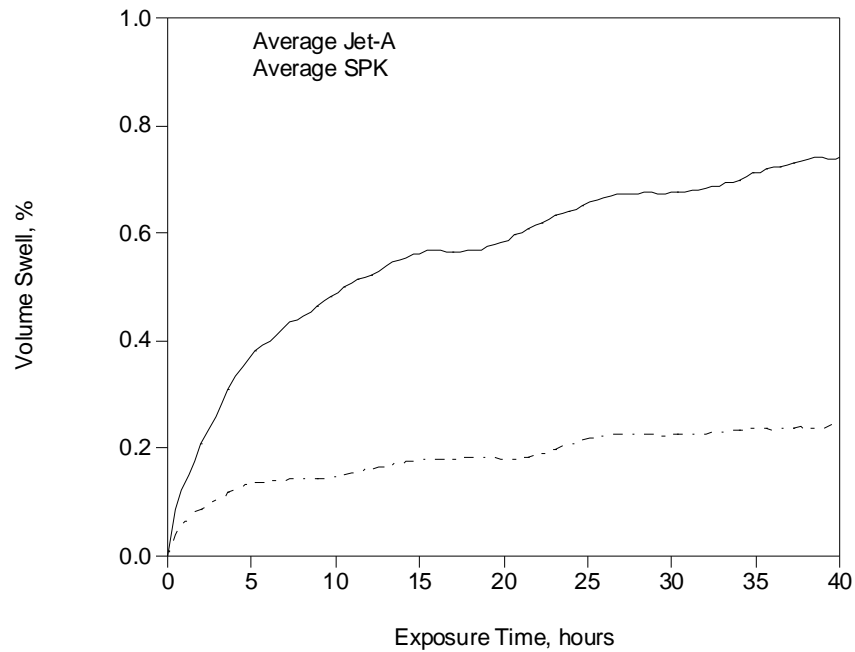


Figure D-1 Average volume swell as a function of time for V0835 at room temperature

Table D-1 Summary of Volume Swell and Mass Fraction of Fuel Absorbed by V0835

| Fuel ID | Aromatics D6379 | Naphs* D6379 | Volume Swell | Mass Fraction |
|---------|-----------------|--------------|--------------|---------------|
| SRI-1 | 8.7% | 0.2% | 0.5% | 0.3% |
| 4597 | 15.0% | 1.9% | 0.7% | 0.6% |
| 5245 | 15.5% | 0.2% | 0.6% | 0.7% |
| 3166 | 17.6% | 2.5% | 0.9% | 0.6% |
| 4598 | 17.6% | 1.4% | 0.6% | 0.7% |
| 4600 | 17.7% | 1.3% | 1.0% | 0.6% |
| 4658 | 17.7% | 1.3% | 0.9% | 0.7% |
| 4626 | 17.9% | 0.6% | 0.4% | 0.6% |
| 5661 | 18.1% | 0.6% | 0.9% | 0.3% |
| 4877 | 19.6% | 0.4% | 0.7% | 0.5% |
| 4599 | 19.9% | 1.4% | 0.6% | 0.6% |
| 3602 | 23.1% | 1.1% | 0.9% | 0.7% |
| SPK-1 | 0.0% | 0.0% | 0.3% | bdl |
| SPK-2 | 0.0% | 0.0% | 0.3% | bdl |
| SPK-3 | 0.0% | 0.0% | 0.3% | 0.3% |
| SPK-4 | 0.0% | 0.0% | 0.2% | 0.2% |

*Naphthalenes

Table D-2 Summary of Polymer-Fuel Partition Coefficients (Kpf) for V0835

| Fuel ID | Aromatics D6379 | Naphs* D6379 | Kpf | | | |
|---------|-----------------|--------------|---------|----------|-------|--------|
| | | | Alkanes | Alkyl Bz | Naph | Naphs* |
| SRI-1 | 8.7% | 0.2% | 0.013 | 0.094 | 0.279 | ** |
| 4597 | 15.0% | 1.9% | 0.011 | 0.091 | 0.255 | 0.151 |
| 5245 | 15.5% | 0.2% | 0.011 | 0.084 | 0.163 | 0.060 |
| 3166 | 17.6% | 2.5% | 0.010 | 0.071 | 0.199 | 0.168 |
| 4598 | 17.6% | 1.4% | 0.010 | 0.079 | 0.160 | 0.104 |
| 4600 | 17.7% | 1.3% | 0.012 | 0.091 | 0.272 | 0.156 |
| 4658 | 17.7% | 1.3% | 0.011 | 0.086 | 0.248 | 0.118 |
| 4626 | 17.9% | 0.6% | 0.010 | 0.079 | 0.209 | 0.095 |
| 5661 | 18.1% | 0.6% | 0.009 | 0.074 | 0.182 | 0.107 |
| 4877 | 19.6% | 0.4% | 0.011 | 0.076 | 0.218 | 0.116 |
| 4599 | 19.9% | 1.4% | 0.013 | 0.107 | 0.327 | 0.160 |
| 3602 | 23.1% | 1.1% | 0.014 | 0.086 | 0.248 | 0.125 |
| | | | | | | |
| Average | 18.2% | 1.2% | 0.011 | 0.085 | 0.230 | 0.124 |
| 90% CI | 1.1% | 0.3% | 0.001 | 0.005 | 0.024 | 0.016 |
| | | | | | | |
| SPK-1 | 0.0% | 0.0% | 0.012 | n.a. | n.a. | n.a. |
| SPK-2 | 0.0% | 0.0% | 0.007 | n.a. | n.a. | n.a. |
| SPK-3 | 0.0% | 0.0% | 0.012 | n.a. | n.a. | n.a. |
| SPK-4 | 0.0% | 0.0% | 0.011 | n.a. | n.a. | n.a. |

*Naphthalenes

**Concentration too low in the fuel for accurate quantification.

***Analysis pending.

Table D-3 Estimated Composition of the Bulk and Absorbed Fuels

| Fuel ID | Bulk Fuel | | | Absorbed Fuel | | |
|---------|-----------|----------|--------|---------------|----------|--------|
| | Alkanes | Alkyl Bz | Naphs* | Alkanes | Alkyl Bz | Naphs* |
| SRI-1 | 91.3% | 8.5% | 0.2% | 59.3% | 40.7% | ** |
| 4597 | 85.0% | 13.1% | 1.9% | 39.2% | 49.0% | 11.8% |
| 5245 | 84.5% | 15.3% | 0.2% | 40.7% | 58.8% | ** |
| 3166 | 82.4% | 15.1% | 2.5% | 35.5% | 46.3% | 18.2% |
| 4598 | 82.4% | 16.2% | 1.4% | 35.8% | 57.7% | 6.5% |
| 4600 | 82.3% | 16.4% | 1.3% | 35.9% | 56.4% | 7.7% |
| 4658 | 82.3% | 16.4% | 1.3% | 36.3% | 57.5% | 6.2% |
| 4626 | 82.1% | 17.3% | 0.6% | 35.4% | 62.0% | 2.6% |
| 5661 | 81.9% | 17.5% | 0.6% | 35.5% | 61.5% | 3.0% |
| 4877 | 80.4% | 19.2% | 0.4% | 37.1% | 61.0% | 1.9% |
| 4599 | 80.1% | 18.5% | 1.4% | 32.2% | 60.9% | 6.9% |
| 3602 | 76.9% | 22.0% | 1.1% | 34.2% | 61.3% | 4.5% |
| | | | | | | |
| Average | 82.6% | 16.3% | 1.1% | 38.1% | 56.1% | 6.9% |
| 90% CI | 98.9% | 0.7% | 0.3% | 0.1% | 0.5% | 2.4% |
| | | | | | | |
| SPK-1 | 100.0% | 0.0% | 0.0% | 100% | 0% | 0% |
| SPK-2 | 100.0% | 0.0% | 0.0% | 100% | 0% | 0% |
| SPK-3 | 100.0% | 0.0% | 0.0% | 100% | 0% | 0% |
| SPK-4 | 100.0% | 0.0% | 0.0% | 100% | 0% | 0% |

*Naphthalenes

**Concentration too low in the fuel for accurate quantification.

***Analysis pending.

5.5 Appendix E PR-1776 Polysulfide Sealant

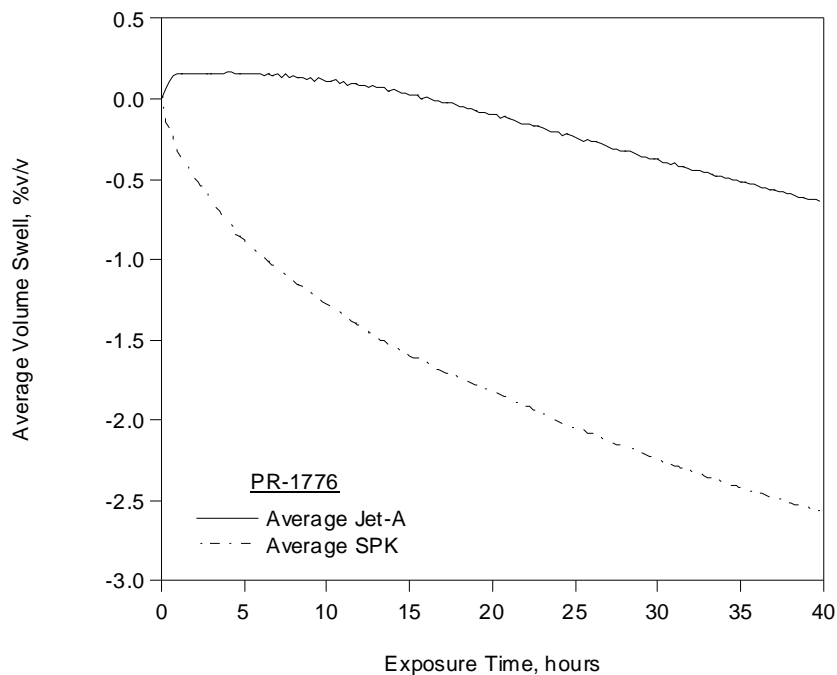


Figure E-1 Average volume swell as a function of time for PR-1776 at room temperature

Table E-1 Summary of Volume Swell and Mass Fraction of Fuel Absorbed by PR-1776

| Fuel ID | Aromatics D6379 | Naphs* D6379 | Volume Swell | Mass Fraction |
|---------|-----------------|--------------|--------------|---------------|
| SRI-1 | 8.7% | 0.2% | -1.6% | 3.3% |
| 4597 | 15.0% | 1.9% | -0.4% | 3.7% |
| 5245 | 15.5% | 0.2% | -1.4% | 3.7% |
| 3166 | 17.6% | 2.5% | -0.1% | 4.7% |
| 4598 | 17.6% | 1.4% | -0.8% | 3.8% |
| 4600 | 17.7% | 1.3% | -0.1% | 4.4% |
| 4658 | 17.7% | 1.3% | -0.6% | 4.4% |
| 4626 | 17.9% | 0.6% | -1.0% | 4.2% |
| 5661 | 18.1% | 0.6% | -0.5% | 4.3% |
| 4877 | 19.6% | 0.4% | -0.7% | 4.2% |
| 4599 | 19.9% | 1.4% | -0.4% | 4.6% |
| 3602 | 23.1% | 1.1% | 0.1% | 4.6% |
| SPK-1 | 0.0% | 0.0% | -2.7% | 2.0% |
| SPK-2 | 0.0% | 0.0% | -3.0% | 2.0% |
| SPK-3 | 0.0% | 0.0% | -2.5% | 2.2% |
| SPK-4 | 0.0% | 0.0% | -2.1% | 1.8% |

*Naphthalenes

Table E-2 Summary of Polymer-Fuel Partition Coefficients (Kpf) for PR-1776

| Fuel ID | Aromatics D6379 | Naphs* D6379 | Kpf | | | |
|---------|-----------------|--------------|---------|----------|-------|--------|
| | | | Alkanes | Alkyl Bz | Naph | Naphs* |
| SRI-1 | 8.7% | 0.2% | 0.039 | 0.143 | ** | ** |
| 4597 | 15.0% | 1.9% | 0.053 | 0.228 | 1.020 | 0.557 |
| 5245 | 15.5% | 0.2% | 0.043 | 0.165 | ** | ** |
| 3166 | 17.6% | 2.5% | 0.051 | 0.200 | 0.931 | 0.484 |
| 4598 | 17.6% | 1.4% | 0.042 | 0.178 | 0.808 | 0.289 |
| 4600 | 17.7% | 1.3% | 0.042 | 0.165 | 0.660 | 0.341 |
| 4658 | 17.7% | 1.3% | 0.045 | 0.169 | 0.761 | 0.356 |
| 4626 | 17.9% | 0.6% | 0.046 | 0.201 | 0.820 | 0.401 |
| 5661 | 18.1% | 0.6% | 0.038 | 0.189 | 0.715 | 0.350 |
| 4877 | 19.6% | 0.4% | 0.041 | 0.169 | 0.688 | 0.344 |
| 4599 | 19.9% | 1.4% | 0.038 | 0.174 | 0.757 | 0.356 |
| 3602 | 23.1% | 1.1% | 0.043 | 0.183 | 0.771 | 0.403 |
| Average | 18.2% | 1.2% | 0.044 | 0.181 | 0.796 | 0.389 |
| 90% CI | 1.1% | 0.3% | 0.002 | 0.011 | 0.061 | 0.042 |
| SPK-1 | 0.0% | 0.0% | 0.032 | n.a. | n.a. | n.a. |
| SPK-2 | 0.0% | 0.0% | 0.038 | n.a. | n.a. | n.a. |
| SPK-3 | 0.0% | 0.0% | 0.040 | n.a. | n.a. | n.a. |
| SPK-4 | 0.0% | 0.0% | 0.029 | n.a. | n.a. | n.a. |

*Naphthalenes **Concentration too low in the fuel for accurate quantification.

Table E-3 Estimated Composition of the Bulk and Absorbed Fuels

| Fuel ID | Bulk Fuel | | | Absorbed Fuel | | |
|---------|-----------|----------|--------|---------------|----------|--------|
| | Alkanes | Alkyl Bz | Naphs* | Alkanes | Alkyl Bz | Naphs* |
| SRI-1 | 91.3% | 8.5% | 0.2% | 74.5% | 25.5% | ** |
| 4597 | 85.0% | 13.1% | 1.9% | 52.6% | 35.0% | 12.4% |
| 5245 | 84.5% | 15.3% | 0.2% | 58.9% | 41.1% | ** |
| 3166 | 82.4% | 15.1% | 2.5% | 50.0% | 35.7% | 14.3% |
| 4598 | 82.4% | 16.2% | 1.4% | 51.2% | 42.8% | 6.0% |
| 4600 | 82.3% | 16.4% | 1.3% | 52.2% | 41.1% | 6.7% |
| 4658 | 82.3% | 16.4% | 1.3% | 53.4% | 39.9% | 6.7% |
| 4626 | 82.1% | 17.3% | 0.6% | 50.5% | 46.3% | 3.2% |
| 5661 | 81.9% | 17.5% | 0.6% | 47.2% | 49.7% | 3.2% |
| 4877 | 80.4% | 19.2% | 0.4% | 49.1% | 48.9% | 2.1% |
| 4599 | 80.1% | 18.5% | 1.4% | 45.3% | 47.4% | 7.3% |
| 3602 | 76.9% | 22.0% | 1.1% | 42.7% | 51.6% | 5.7% |
| Average | 82.6% | 16.3% | 1.1% | 52.3% | 42.1% | 6.8% |
| 90% CI | 98.9% | 0.7% | 0.3% | 0.2% | 1.1% | 5.7% |
| SPK-1 | 100.0% | 0.0% | 0.0% | 100.0% | 0.0% | 0.0% |
| SPK-2 | 100.0% | 0.0% | 0.0% | 100.0% | 0.0% | 0.0% |
| SPK-3 | 100.0% | 0.0% | 0.0% | 100.0% | 0.0% | 0.0% |
| SPK-4 | 100.0% | 0.0% | 0.0% | 100.0% | 0.0% | 0.0% |

*Naphthalenes **Concentration too low in the fuel for accurate quantification.

5.6 Appendix F PR-1828 Polythioether Sealant

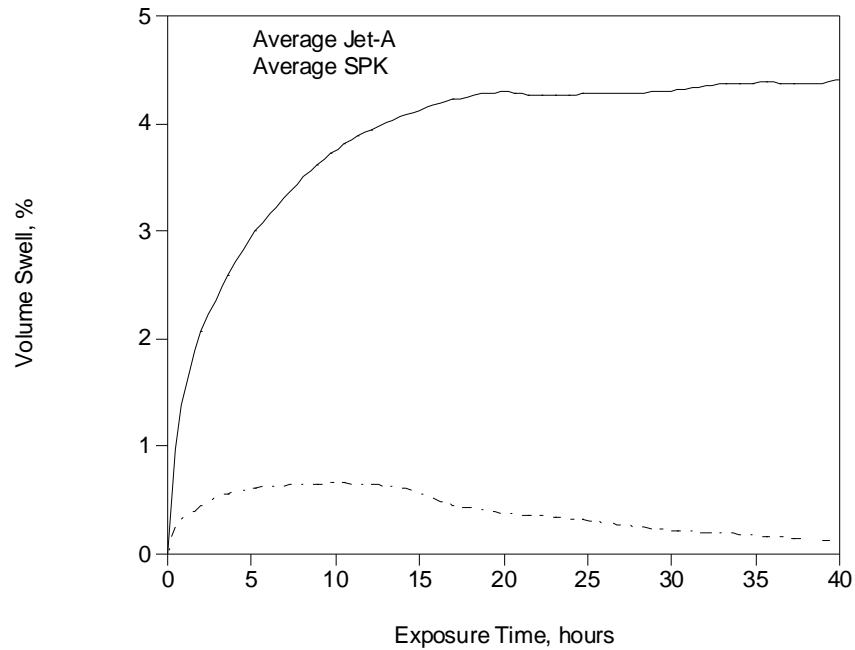


Figure F-1 Average volume swell as a function of time for PR-1828 at room temperature

Table F-1 Summary of Volume Swell and Mass Fraction of Fuel Absorbed by PR-1828

| Fuel ID | Aromatics D6379 | Naphs* D6379 | Volume Swell | Mass Fraction |
|---------|-----------------|--------------|--------------|---------------|
| SRI-1 | 8.7% | 0.2% | 3.0% | 2.8% |
| 4597 | 15.0% | 1.9% | 4.9% | 4.3% |
| 5245 | 15.5% | 0.2% | 3.3% | 3.7% |
| 3166 | 17.6% | 2.5% | 5.3% | 4.7% |
| 4598 | 17.6% | 1.4% | 4.2% | 3.6% |
| 4600 | 17.7% | 1.3% | 4.6% | 4.2% |
| 4658 | 17.7% | 1.3% | 4.2% | 4.1% |
| 4626 | 17.9% | 0.6% | 3.8% | 3.7% |
| 5661 | 18.1% | 0.6% | 4.9% | 4.4% |
| 4877 | 19.6% | 0.4% | 4.2% | 3.8% |
| 4599 | 19.9% | 1.4% | 4.7% | 4.0% |
| 3602 | 23.1% | 1.1% | 5.5% | 4.9% |
| SPK-1 | 0.0% | 0.0% | -0.1% | 1.2% |
| SPK-2 | 0.0% | 0.0% | 0.3% | 1.4% |
| SPK-3 | 0.0% | 0.0% | 0.3% | 1.4% |
| SPK-4 | 0.0% | 0.0% | 0.2% | 1.3% |

*Naphthalenes

Table F-2 Summary of Polymer-Fuel Partition Coefficients (Kpf) for PR-1828

| Fuel ID | Aromatics D6379 | Naphs* D6379 | Kpf | | | |
|---------|-----------------|--------------|---------|----------|-------|--------|
| | | | Alkanes | Alkyl Bz | Naph | Naphs* |
| SRI-1 | 8.7% | 0.2% | 0.023 | 0.164 | ** | ** |
| 4597 | 15.0% | 1.9% | 0.027 | 0.188 | 0.674 | 0.447 |
| 5245 | 15.5% | 0.2% | 0.032 | 0.217 | ** | ** |
| 3166 | 17.6% | 2.5% | 0.030 | 0.201 | 0.741 | 0.416 |
| 4598 | 17.6% | 1.4% | 0.027 | 0.196 | 0.919 | 0.372 |
| 4600 | 17.7% | 1.3% | 0.029 | 0.181 | 0.758 | 0.408 |
| 4658 | 17.7% | 1.3% | 0.026 | 0.176 | 0.703 | 0.376 |
| 4626 | 17.9% | 0.6% | 0.030 | 0.185 | 0.882 | 0.456 |
| 5661 | 18.1% | 0.6% | 0.036 | 0.219 | 0.844 | 0.457 |
| 4877 | 19.6% | 0.4% | 0.029 | 0.176 | 0.707 | 0.434 |
| 4599 | 19.9% | 1.4% | 0.026 | 0.174 | 0.758 | 0.391 |
| 3602 | 23.1% | 1.1% | 0.034 | 0.190 | 0.767 | 0.439 |
| Average | 18.2% | 1.2% | 0.029 | 0.189 | 0.775 | 0.419 |
| 90% CI | 1.1% | 0.3% | 0.002 | 0.008 | 0.042 | 0.017 |
| SPK-1 | 0.0% | 0.0% | 0.025 | n.a. | n.a. | n.a. |
| SPK-2 | 0.0% | 0.0% | 0.027 | n.a. | n.a. | n.a. |
| SPK-3 | 0.0% | 0.0% | 0.025 | n.a. | n.a. | n.a. |
| SPK-4 | 0.0% | 0.0% | 0.032 | n.a. | n.a. | n.a. |

*Naphthalenes **Concentration too low in the fuel for accurate quantification.

Table F-3 Estimated Composition of the Bulk and Absorbed Fuels

| Fuel ID | Bulk Fuel | | | Absorbed Fuel | | |
|---------|-----------|----------|--------|---------------|----------|--------|
| | Alkanes | Alkyl Bz | Naphs* | Alkanes | Alkyl Bz | Naphs* |
| SRI-1 | 91.3% | 8.5% | 0.2% | 74.5% | 25.5% | ** |
| 4597 | 85.0% | 13.1% | 1.9% | 52.6% | 35.0% | 12.4% |
| 5245 | 84.5% | 15.3% | 0.2% | 58.9% | 41.1% | ** |
| 3166 | 82.4% | 15.1% | 2.5% | 50.0% | 35.7% | 14.3% |
| 4598 | 82.4% | 16.2% | 1.4% | 51.2% | 42.8% | 6.0% |
| 4600 | 82.3% | 16.4% | 1.3% | 52.2% | 41.1% | 6.7% |
| 4658 | 82.3% | 16.4% | 1.3% | 53.4% | 39.9% | 6.7% |
| 4626 | 82.1% | 17.3% | 0.6% | 50.5% | 46.3% | 3.2% |
| 5661 | 81.9% | 17.5% | 0.6% | 47.2% | 49.7% | 3.2% |
| 4877 | 80.4% | 19.2% | 0.4% | 49.1% | 48.9% | 2.1% |
| 4599 | 80.1% | 18.5% | 1.4% | 45.3% | 47.4% | 7.3% |
| 3602 | 76.9% | 22.0% | 1.1% | 42.7% | 51.6% | 5.7% |
| Average | 82.6% | 16.3% | 1.1% | 52.3% | 42.1% | 6.8% |
| 90% CI | 98.9% | 0.7% | 0.3% | 0.2% | 1.1% | 5.7% |
| SPK-1 | 100.0% | 0.0% | 0.0% | 100.0% | 0.0% | 0.0% |
| SPK-2 | 100.0% | 0.0% | 0.0% | 100.0% | 0.0% | 0.0% |
| SPK-3 | 100.0% | 0.0% | 0.0% | 100.0% | 0.0% | 0.0% |
| SPK-4 | 100.0% | 0.0% | 0.0% | 100.0% | 0.0% | 0.0% |

*Naphthalenes **Concentration too low in the fuel for accurate quantification.

5.7 Appendix G BMS 10-20 Epoxy Fuel Tank Coating

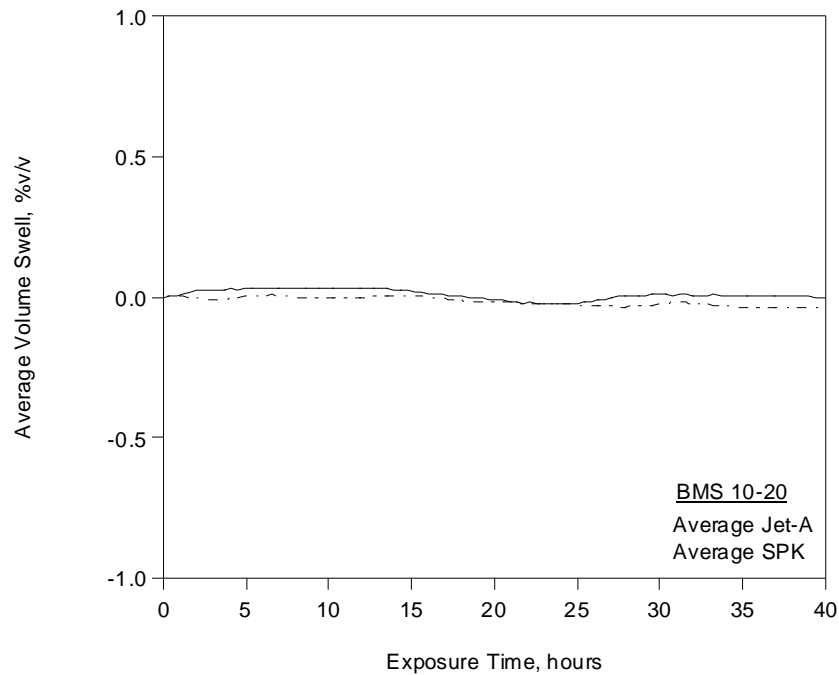


Figure G-1 Average volume swell as a function of time for BMS 10-20 at room temperature

Table G-1 Summary of Volume Swell and Mass Fraction of Fuel Absorbed by BMS 10-20

| Fuel ID | Aromatics D6379 | Naphs D6379 | Volume Swell | Mass Fraction |
|---------|-----------------|-------------|--------------|---------------|
| SRI-1 | 8.7% | 0.2% | 0.1% | * |
| 4597 | 15.0% | 1.9% | -0.1% | * |
| 5245 | 15.5% | 0.2% | 0.0% | * |
| 3166 | 17.6% | 2.5% | 0.0% | * |
| 4598 | 17.6% | 1.4% | 0.0% | * |
| 4600 | 17.7% | 1.3% | 0.0% | * |
| 4658 | 17.7% | 1.3% | 0.1% | * |
| 4626 | 17.9% | 0.6% | 0.0% | * |
| 5661 | 18.1% | 0.6% | 0.1% | * |
| 4877 | 19.6% | 0.4% | 0.0% | * |
| 4599 | 19.9% | 1.4% | 0.1% | * |
| 3602 | 23.1% | 1.1% | -0.1% | * |
| SPK-1 | 0.0% | 0.0% | -0.1% | * |
| SPK-2 | 0.0% | 0.0% | -0.1% | * |
| SPK-3 | 0.0% | 0.0% | 0.0% | * |
| SPK-4 | 0.0% | 0.0% | 0.0% | * |

*The mass of fuel absorbed was too small to be accurately measured by TGA

5.8 Appendix H BMS 10-123 Epoxy Fuel Tank Coating

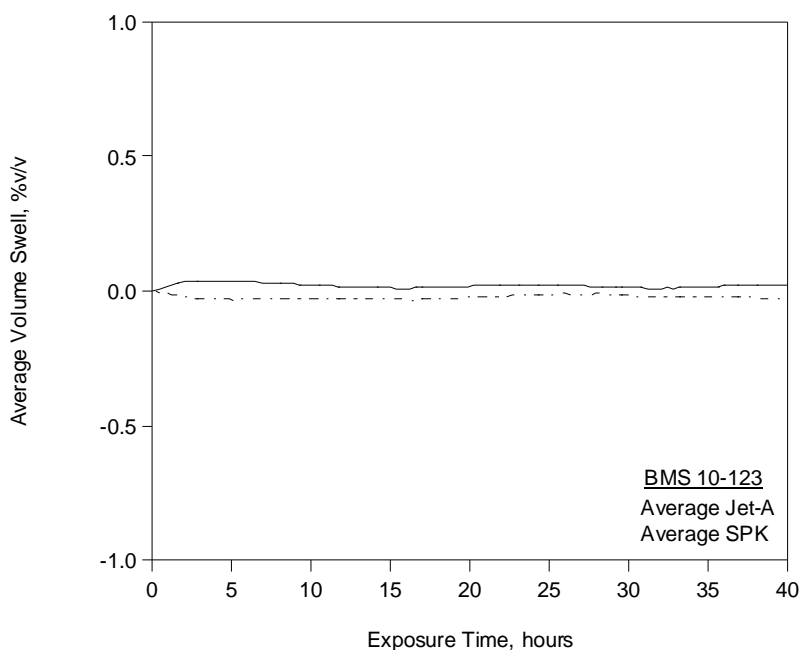


Figure H-1 Average volume swell as a function of time for BMS 10-123 at room temperature

Table H-1 Summary of Volume Swell and Mass Fraction of Fuel Absorbed by BMS 10-123

| Fuel ID | Aromatics D6379 | Naphs D6379 | Volume Swell | Mass Fraction |
|---------|-----------------|-------------|--------------|---------------|
| SRI-1 | 8.7% | 0.2% | 0.0% | * |
| 4597 | 15.0% | 1.9% | 0.0% | * |
| 5245 | 15.5% | 0.2% | 0.1% | * |
| 3166 | 17.6% | 2.5% | 0.2% | * |
| 4598 | 17.6% | 1.4% | 0.0% | * |
| 4600 | 17.7% | 1.3% | 0.0% | * |
| 4658 | 17.7% | 1.3% | 0.0% | * |
| 4626 | 17.9% | 0.6% | -0.1% | * |
| 5661 | 18.1% | 0.6% | 0.0% | * |
| 4877 | 19.6% | 0.4% | -0.1% | * |
| 4599 | 19.9% | 1.4% | 0.0% | * |
| 3602 | 23.1% | 1.1% | 0.1% | * |
| SPK-1 | 0.0% | 0.0% | 0.0% | * |
| SPK-2 | 0.0% | 0.0% | 0.0% | * |
| SPK-3 | 0.0% | 0.0% | -0.1% | * |
| SPK-4 | 0.0% | 0.0% | 0.0% | * |

*The mass of fuel absorbed was too small to be accurately measured by TGA

5.9 Appendix I Nylon (6,6) Film

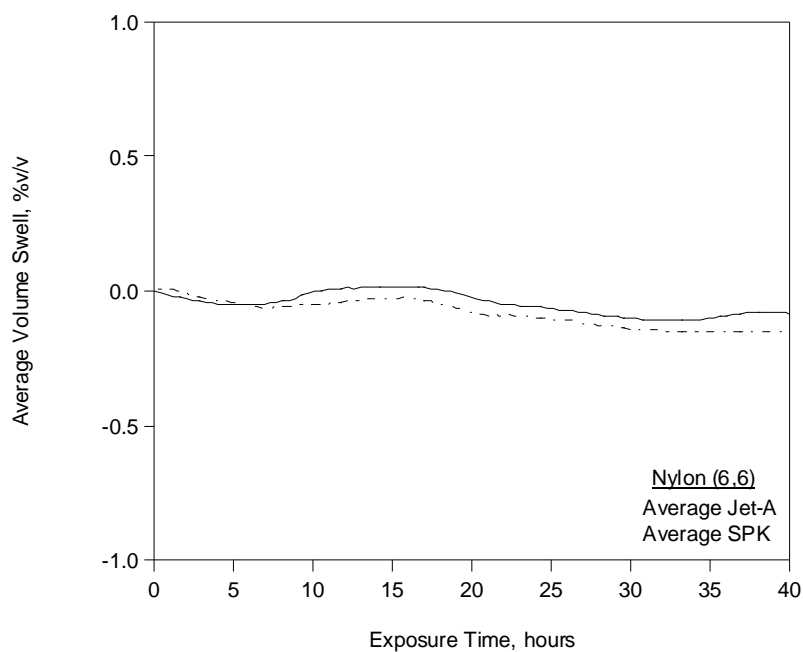


Figure I-1 Average volume swell as a function of time for Nylon (6,6) at room temperature

Table I-1 Summary of Volume Swell and Mass Fraction of Fuel Absorbed by Nylon (6,6)

| Fuel ID | Aromatics D6379 | Naphs D6379 | Volume Swell | Mass Fraction |
|---------|-----------------|-------------|--------------|---------------|
| SRI-1 | 8.7% | 0.2% | 0.0% | * |
| 4597 | 15.0% | 1.9% | -0.1% | * |
| 5245 | 15.5% | 0.2% | -0.1% | * |
| 3166 | 17.6% | 2.5% | -0.1% | * |
| 4598 | 17.6% | 1.4% | -0.1% | * |
| 4600 | 17.7% | 1.3% | -0.1% | * |
| 4658 | 17.7% | 1.3% | 0.0% | * |
| 4626 | 17.9% | 0.6% | 0.0% | * |
| 5661 | 18.1% | 0.6% | -0.2% | * |
| 4877 | 19.6% | 0.4% | -0.1% | * |
| 4599 | 19.9% | 1.4% | -0.1% | * |
| 3602 | 23.1% | 1.1% | -0.2% | * |
| SPK-1 | 0.0% | 0.0% | -0.2% | * |
| SPK-2 | 0.0% | 0.0% | -0.1% | * |
| SPK-3 | 0.0% | 0.0% | -0.2% | * |
| SPK-4 | 0.0% | 0.0% | -0.1% | * |

*The mass of fuel absorbed was too small to be accurately measured by TGA

5.10 Appendix J Kapton® Film

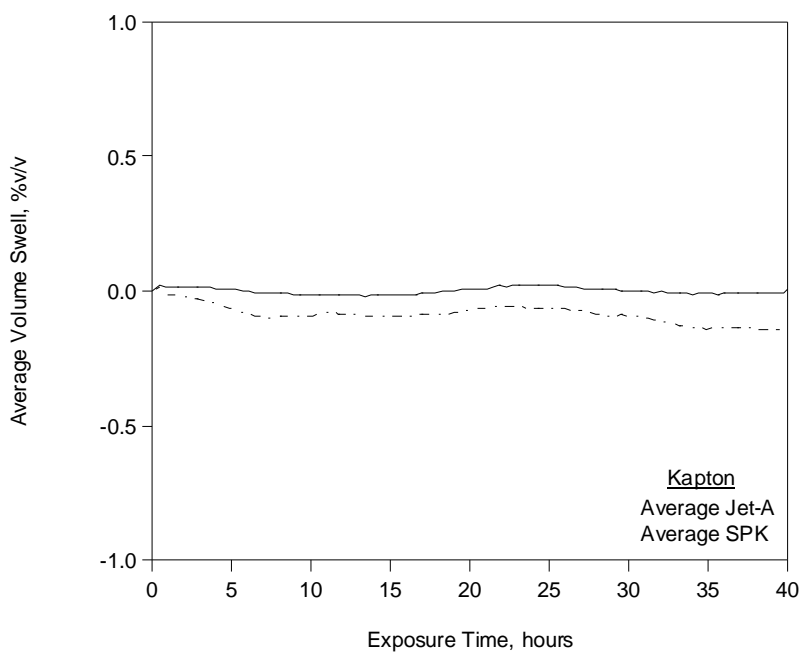


Figure J-1 Average volume swell as a function of time for Kapton® at room temperature

Table J-1 Summary of Volume Swell and Mass Fraction of Fuel Absorbed by Kapton

| Fuel ID | Aromatics D6379 | Naphs D6379 | Volume Swell | Mass Fraction |
|---------|-----------------|-------------|--------------|---------------|
| SRI-1 | 8.7% | 0.2% | 0.0% | * |
| 4597 | 15.0% | 1.9% | -0.1% | * |
| 5245 | 15.5% | 0.2% | 0.1% | * |
| 3166 | 17.6% | 2.5% | 0.0% | * |
| 4598 | 17.6% | 1.4% | 0.0% | * |
| 4600 | 17.7% | 1.3% | 0.0% | * |
| 4658 | 17.7% | 1.3% | 0.1% | * |
| 4626 | 17.9% | 0.6% | -0.2% | * |
| 5661 | 18.1% | 0.6% | 0.0% | * |
| 4877 | 19.6% | 0.4% | 0.0% | * |
| 4599 | 19.9% | 1.4% | 0.1% | * |
| 3602 | 23.1% | 1.1% | 0.0% | * |
| SPK-1 | 0.0% | 0.0% | -0.1% | * |
| SPK-2 | 0.0% | 0.0% | -0.1% | * |
| SPK-3 | 0.0% | 0.0% | -0.3% | * |
| SPK-4 | 0.0% | 0.0% | -0.1% | * |

*The mass of fuel absorbed was too small to be accurately measured by TGA

5.11 Appendix K JP-8 to FT Transition

Prior, related studies were conducted by UDRI, using JP-8 for similar materials as used in this study. As shown in Figure K-1, nitrile rubber, fluorosilicone, and fluorocarbon were tested out to over 150 hours from dry to JP-8, after which they were transitioned to 100% FT fuel, and examined to over 300 hours. These results indicate that the aromatics' impact on nitrile rubber in a fuel-switching scenario should be considered for further evaluation. Note that these tests were conducted using approximately 1/3rd sections of whole O-rings as compared to the 1mm slices of O-rings used in this study. Earlier work has shown that using the 1mm slices increased the rate of volume swell (by virtue of a higher surface to volume ratio), but did not affect the extent of volume swell. This permitted the exposure time to be shortened from 150 hours to 40 hours in the present study where the temporal behavior was not considered as a primary factor.

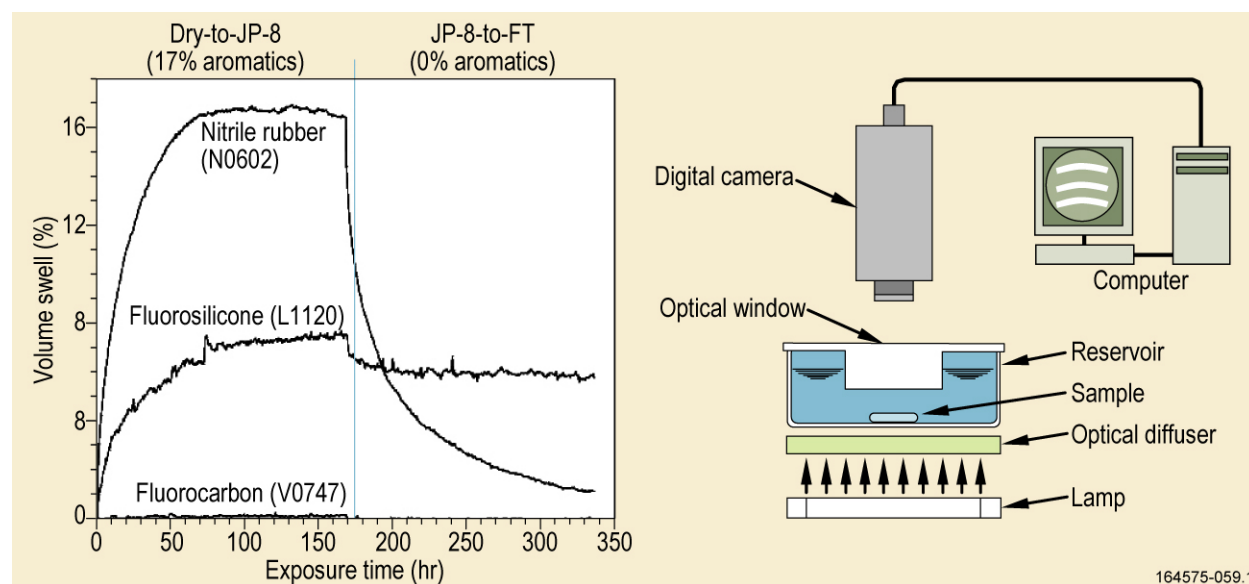


Figure K-1 Volume swell for JP-8 to FT Transition